

A new species of barred *Sternopygus* (Gymnotiformes: Sternopygidae) from the Orinoco River



Correspondence:
Kevin T. Torgersen
kevinorgersen@gmail.com

¹Kevin T. Torgersen¹, ²Aleidy M. Galindo-Cuervo²,
¹Roberto E. Reis² and ¹James S. Albert¹

Submitted September 11, 2022

Accepted March 13, 2023

by William Crampton

Epub April 14, 2023

A new species of *Sternopygus* is described from the Orinoco River of Venezuela using traditional methods of morphometrics and meristics, and micro-computed tomography (micro-CT) imaging for osteological analysis. The new species is readily separated from all congeners in having broad, vertical pigment bars that extend from the mid-dorsum to the ventral margin of the pterygiophores. A similar color pattern, characterized by subtle differences in the densities and sizes of chromatophores, is also present in juveniles of *S. obtusirostris* from the Amazon River, juveniles of *S. sabaji* from rivers of the Guiana Shield, and *S. astrabes* from clearwater and blackwater terra firme streams of lowlands around the Guiana Shield. The new species further differs from other congeners in the Orinoco basin by having a reduced humeral pigment blotch with poorly defined margins, a proportionally smaller head, a longer body cavity, a more slender body shape in lateral profile, and in having vertical pigment bars that extend ventrally to the pterygiophores (*vs.* pigment saddles not reaching the pterygiophores). The description of this species raises to three the number of *Sternopygus* species in the Orinoco basin, and to 11 the total number of *Sternopygus* species.

Keywords: Biodiversity, Computed tomography, Knifefish, Morphometrics, Taxonomy.



Online version ISSN 1982-0224

Print version ISSN 1679-6225

Neotrop. Ichthyol.
vol. 21, no. 1, Maringá 2023

¹ Department of Biology, University of Louisiana at Lafayette, 70503 Lafayette, LA, USA. (KTT) kevinorgersen@gmail.com (corresponding author), (JSA) jalbert@louisiana.edu.

² Pontificia Universidade Católica do Rio Grande do Sul, Av. Ipiranga, 6681, 90619-900 Porto Alegre, RS, Brazil. (AMGC) aleidyga@hotmail.com, (RER) reis@puers.br.

Se describe una nueva especie de *Sternopygus* del río Orinoco de Venezuela utilizando métodos tradicionales de morfometría y métrica, y microtomografía computarizada (micro-CT) para análisis osteológico. La nueva especie se distingue fácilmente de todos los congéneres por tener barras de pigmento verticales anchas que se extienden desde la parte media del dorso hasta el margen ventral de los pterigióforos. Un patrón de color similar, caracterizado por diferencias sutiles en las densidades y tamaños de los cromatóforos, también está presente en juveniles de *S. obtusirostris* del río Amazonas, juveniles de *S. sabaji* de ríos del Escudo Guayanés y *S. astrabes* de aguas claras y arroyos de tierra firme de aguas negras de las tierras bajas alrededor del Escudo Guayanés. La nueva especie se diferencia aún más de otros congéneres en la cuenca del Orinoco por tener una mancha de pigmento humeral reducida con márgenes mal definidos, una cabeza proporcionalmente más pequeña, una cavidad corporal más larga, una forma corporal más delgada en el perfil lateral y por tener barras de pigmento verticales que extendirse ventralmente a los pterigióforos (frente a las monturas de pigmentos que no llegan a los pterigióforos). La descripción de esta especie eleva a tres el número de especies de *Sternopygus* en la cuenca del Orinoco y a 11 el número total de especies de *Sternopygus*.

Palabras clave: Biodiversidad, Morfometría, Pez cuchillo, Taxonomía, Tomografía computarizada.

INTRODUCTION

With more than 1,000 described fish species, the Orinoco basin is one of the world's hotspots of freshwater fish biodiversity (Lasso *et al.*, 2004, 2011, 2016; Albert *et al.*, 2011, 2020). Gymnotiform electric fishes (also called knifefishes) are an important component of the taxonomic and functional diversity of the Orinoco fauna (Lundberg *et al.*, 1987; Albert, Crampton, 2005). Taxonomic knowledge of gymnotiform diversity in the Orinoco River has increased dramatically since the 1980s (*e.g.*, Mago-Leccia, Zaret, 1978; Mago-Leccia *et al.*, 1985, 1994; Lundberg, Stager, 1985; Lundberg, Mago-Leccia, 1986; de Santana, Crampton, 2011; Crampton *et al.*, 2016). The results of these and other studies have more than tripled the number of described gymnotiform species known from the Orinoco basin from 20 to 65 over a period of 35 years (Machado-Allison, 1987; Maldonado-Ocampo, Albert, 2003; Van der Sleen, Albert, 2017; Peixoto, Waltz, 2017). These recent advances in our knowledge of gymnotiform species richness and species limits have improved our understanding of ecological and evolutionary processes (Marrero, Winemiller, 1993; Barbarino Duque, Winemiller, 2003; Winemiller, 2004; Lovejoy *et al.*, 2010).

“Longtail electric fishes” of the genus *Sternopygus* Müller & Troschel, 1846 are widely distributed across the lowland river basins (<250 m elevation) of the humid Neotropics, from northern Argentina to Panama (Hulen *et al.*, 2005; Waltz, Albert, 2017). Currently, 10 *Sternopygus* species are recognized as valid (Tab. 1; Hulen *et al.*, 2005; Torgersen, Albert, 2022). However, differences in morphology (Albert, Fink, 1996), karyotypes

TABLE 1 | Summary of all valid species of *Sternopygus* with information regarding primary type specimens and locality drainage for each species. Country of collection of primary types given in parenthesis.

Species	Holotype	Type drainage (Country)
<i>Sternopygus aequilabiatus</i> (Humboldt, 1805)	Whereabouts unknown	Magdalena (Colombia)
<i>Sternopygus arenatus</i> Eydoux & Souleyet, 1841	MNHN 0000-3809 (2 syntypes)	Guayaquil (Ecuador)
<i>Sternopygus astrabes</i> Mago-Leccia, 1994	MBUCV-V-14182	Orinoco (Venezuela)
<i>Sternopygus branco</i> Crampton, Hulen & Albert, 2004	MCP 32451	Amazonas (Brazil)
<i>Sternopygus dariensis</i> Meek & Hildebrand, 1913	FMNH 8949	Tuira (Panama)
<i>Sternopygus macrurus</i> (Bloch & Schneider, 1801)	ZMB 8701 (syntype, stuffed)	Unknown (Brazil)
<i>Sternopygus obtusirostris</i> Steindachner, 1881	MCZ 9413 (lectotype)	Amazonas (Brazil)
<i>Sternopygus pejeraton</i> Schultz, 1949	USNM 121752	Maracaibo (Venezuela)
<i>Sternopygus sabaji</i> Torgersen & Albert, 2022	ANSP 208090	Maroni (Suriname)
<i>Sternopygus</i> n. sp. (in this study)	ANSP 209718	Orinoco (Venezuela)
<i>Sternopygus xingu</i> Albert & Fink, 1996	MZUSP 48374	Xingu (Brazil)

(Santos Silva *et al.*, 2008), and gene sequences (Maldonado-Ocampo, 2011) indicate that museum collections contain additional undescribed species. Only two *Sternopygus* species are known from the Orinoco basin: *S. macrurus* (Bloch & Schneider, 1801) (type locality unknown but in “Brazil”), and *S. astrabes* Mago-Leccia, 1994, which was described from a clearwater tributary of the upper Orinoco River. *Sternopygus macrurus* exhibits the broadest geographic distribution of all nominal gymnotiform species, with specimens ascribed to this species recorded from Pacific slope basins of Colombia to the Pampas of Argentina (Eigenmann, Ward, 1905; Eigenmann, Allen, 1942; Albert, Fink, 1996). *Sternopygus macrurus* is also thought to be among the most ecologically tolerant of all gymnotiform species, inhabiting water bodies of varying water chemistry (clearwater, blackwater, whitewater) and flow (riffles and runs) in lowland forests, seasonal floodplains, and even estuarine environments (Crampton, 1996, 1998a,b; Fernandes, 1999; Marceniuk *et al.*, 2017). Due to its widespread distribution, unknown type locality, and conserved morphology, *S. macrurus* has long been a “wastebasket” taxon into which many specimens in museum collections have been ascribed.

Fishes ascribed to *Sternopygus* can be diagnosed from all other sternopygids by the following characters: (1) relatively larger gape (Mago-Leccia, 1978); (2) large branchial opening (Mago-Leccia, 1978); (3) long, evenly curved maxilla; (4) anterior process of maxilla extends as a narrow hook-like process (Lundberg, Mago-Leccia, 1986); (5) dorsal portion of ventral ethmoid elongate (Albert, Fink, 1996); (6) post-temporal fossa present between pterotic and epioccipital bones (Lundberg, Mago-Leccia, 1986); (7) gill rakers composed of three bony elements, the middle one with 3–10 small teeth (Mago-Leccia, 1978); (8) gill rakers not attached to branchial arches (Albert, Fink, 1996); (9) gap between parapophyses of second vertebra; (10) unossified post cleithrum (Albert, Fink, 1996); (11) long body cavity, with 18–30 precaudal vertebrae (Albert, Fink, 1996); (12) long anal fin with 170–340 rays, (13) unbranched anal-fin rays (Fink, Fink, 1981); (14) developmental origin of adult electric organ from both hypaxial and epaxial muscles

(Unguez, Zakon, 1998; Albert, 2001); (15) absence of jamming avoidance response (Heiligenberg, 1991; Albert, 2001); (16) presence of a ‘medial cephalic fold’ (Triques, 2000), defined as a ridge of ectodermal tissue extending from the ventral limit of the opercular opening anteromedially to the branchial isthmus. Most *Sternopygus* species attain medium to large body sizes (40–50 cm Total Length (TL)), except the more diminutive *S. astrabes* which grows to about 20 cm TL. Most *Sternopygus* species are nocturnal predators of small animals (e.g, insect larvae, crustaceans) and occur in multiple habitats, including small streams, river margins, and deep river channels (Crampton *et al.*, 2004a; Crampton, 2007, 2011; Brejão *et al.*, 2013).

Most *Sternopygus* species share a similar color pattern with a base color composed of small, densely arranged gray chromatophores. Some species have a dark humeral blotch with variable contrast to the background coloration, and a distinctive yellow or white longitudinal stripe extending between the hypaxial and pterygiophore muscles on the posterior third of the body. These aspects of coloration are variable within and among nominal species and are sometimes absent, with some specimens ranging in color from deep black to pinkish white. At least three valid *Sternopygus* species possess a distinctive color pattern composed of 1–4 broad, dark vertical bars or saddles across the dorsal midline at some stage in their ontogeny: *S. astrabes*, *S. obtusirostris* Steindachner, 1881, *S. sabaji* Torgersen & Albert, 2022 (Fig. 1; Mago-Leccia, 1994; Crampton *et al.*, 2004b; Torgersen, Albert, 2022). The monophyly, species limits, variation, and species richness of species with broad vertical pigment bars or saddles remains poorly understood and these topics are not addressed here.

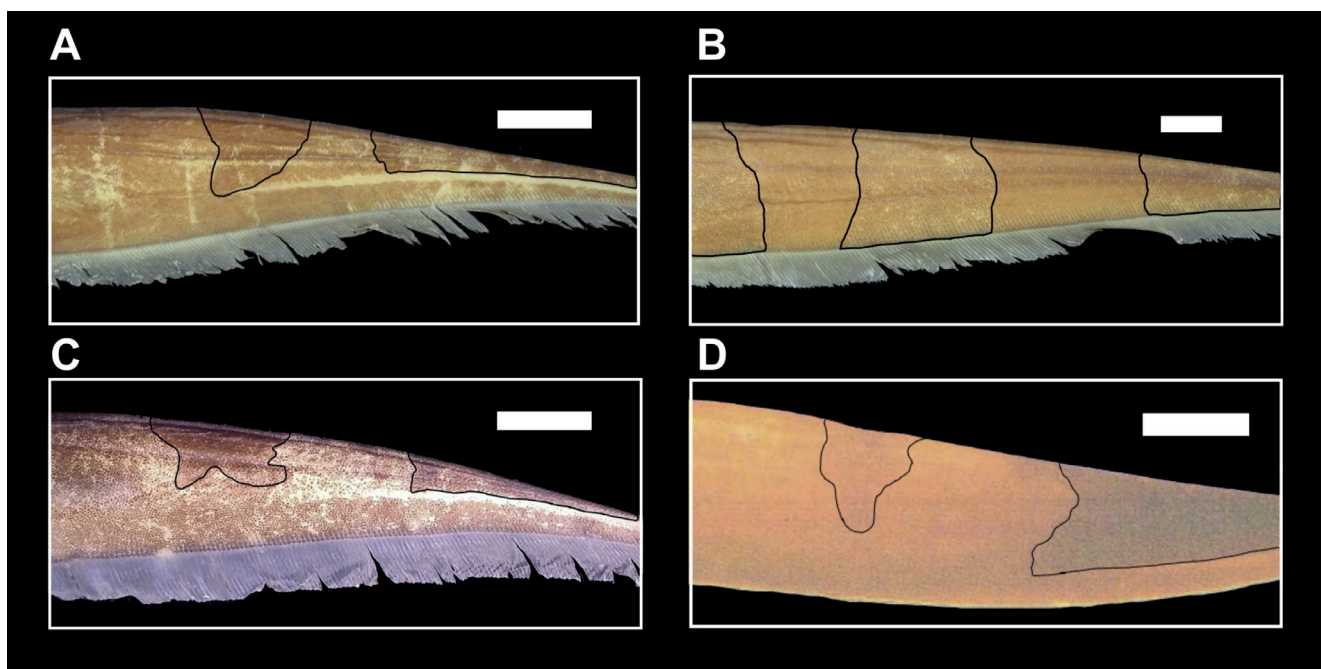


FIGURE 1 | Four species of barred *Sternopygus*. **A.** *Sternopygus astrabes*, ANSP 162663 (189 mm TL); **B.** *Sternopygus* n. sp., ANSP 160357 (284 mm TL, paratype); **C.** Juvenile *Sternopygus sabaji*, ANSP 189018 (146 mm TL); **D.** Juvenile *Sternopygus obtusirostris*, INPA 15787 (180 mm TL), photo taken at night from Crampton *et al.* (2004b). Dark outlines added to bars/saddles in all photos for emphasis. Scale bars = 1 cm.

Here we describe a new species of barred *Sternopygus* from the lower Orinoco basin of Venezuela, bringing the total number of species in the genus to 11, the number of species known in the Orinoco basin to three, the number of species in the Guiana Shield region to four, and the number of *Sternopygus* species possessing dark vertical bars to four.

MATERIAL AND METHODS

A total of 46 specimens of the new species described herein were identified from museum lots collected in the lower Orinoco drainage of Venezuela between 1985 and 2010, with most specimens collected specifically from the confluence of the Orinoco and Caura rivers by L. Aguana, B. Chernoff, R. Royero, and W. Saul. Only specimens collected near the confluence of the Orinoco and Caura rivers were included in the type series. We were unable to deposit type specimens in Venezuela because of the ongoing political and economic instability. No animal experimentation or collection permits or approvals were necessary for the completion of this work.

Morphometric measurements followed Hulen *et al.* (2005). We used digital calipers and an ocular micrometer attached to an Olympus SZX12 dissecting microscope, measuring point-to-point linear distances from standard landmarks to the nearest 0.01 mm on the left side of the body when possible.

We measured: (1) length to the end of the anal fin (LEA) measured as the length from the tip of the snout (anterior margin of upper jaw at mid-axis of body) to the end of last anal-fin ray; (2) anal-fin length (AFL), measured from the origin of the anal fin at the isthmus to the end of the fin; (3) caudal appendage (CA), measured as the distance from the last anal-fin ray to the distal end of the caudal filament. Note: the CA in sternopygid fishes is often damaged, entirely missing, or in a variable state of regeneration. Therefore, the values reported here are not considered to have diagnostic value; (4) body depth (BD), measured as a vertical distance from the origin of the anal fin to the dorsal body border, (5) body width (BW), measured as body width at the origin of the anal-fin; (6) head length (HL), measured from the posterior margin of the bony opercle to the tip of the snout; (7) postorbital head length (PO), measured from the posterior margin of the bony opercle to posterior rim of free orbital margin of eye; (8) preorbital head length (PR), measured from the anterior rim of the orbital free margin to tip of snout; (9) eye diameter (ED), measured as the horizontal distance between the anterior and posterior rims of the free orbital margin; (10) interorbital length (IO), measured between the dorsomedial margins of the free orbital margin; (11) inter-narial distance (NN), measured from the posterior margin of the anterior nares to the anterior margin of the posterior nares; (12) mouth width (MW), measured as the horizontal distance of the gape at the rictus; (13) branchial opening (BO) measured as the distance from the posterodorsal to anteroventral extent of the skin fold of the branchial opening along the anterior margin; (14) head depth (HD), measured as the vertical distance at the nape to ventral body border with the lateral line held horizontal; (15) head width (HW) measured as the width at nape; (16) preanal distance (PA), measured from the origin of the anal fin to the posterior margin of anus; (17) pectoral-fin length (P1), measured from the dorsal border of fin base where it contacts the cleithrum to the tip of the longest ray. Morphometric data were standardized for size by reporting values as a percent of HL, except in HL %, BD %, BW %, and CA %, which are reported as a percent of LEA.

We assessed a body-shape tapering ratio (TR) as the ratio of BD at 75% LEA divided by BD at 25% LEA (Fig. 2). To reduce the effects of allometry, morphometric measurements used in the diagnosis were limited to morphologically mature specimens (more than 50% maximum known TL). Specimens that are damaged or with incompletely regenerated tails were excluded from analysis. Diagnostic trait values are reported as non-overlapping range values or range values within the 95% confidence interval (*i.e.*, overlap less than 5.0%). Additional traits that are useful in identifying specimens of the new species are reported in the Diagnosis. The sex of six specimens was assessed by direct examination of gonads following Waddell, Crampton (2018) and Waddell *et al.* (2019).

Meristic counts also follow Hulen *et al.* (2005) and include: (1) anal-fin rays (AFR); (2) pectoral-fin rays (P1R) including all branched and unbranched rays; (3) precaudal vertebrae (PCV) including the four vertebrae that compose the Weberian apparatus; (4) scales above the lateral line (SAL) counted along a vertical line at the end of the body cavity; (5) scales below the lateral line (SBL) from the same point as SAL to the base of the anal-fin pterygiophores; (6) scales over the pterygiophores (SOP) counted from the same point as SAL at the base of the anal-fin pterygiophores to the anal-fin ventral border.

Micro-computed tomography (micro-CT) scans were made of 10 specimens from the type series of the new species using a Bruker SkyScan1273 with an x-ray source voltage of 65 kV. Only the head region, defined as the part of the body extending from the tip of the snout to a point between vertebrae 4–8 along the longitudinal axis of the specimens were scanned due to exceedingly large file sizes resulting from full-body scans and the relatively low return of information from scans past the body cavity. Osteological observations were made from 3D renderings of the micro-CT scans in the freeware Slicer (Fedorov *et al.*, 2012) after being prepared in Fiji/ImageJ (Schindelin *et al.*, 2012) following Buser *et al.* (2020). Precaudal vertebrae were counted from x-rays obtained from the CT scanner. Figures featuring images of 3D renderings were accomplished by taking screen captures of the renderings generated in Slicer before preparing them in additional photo editing software. The package ‘ggridges’ was used to create Ridgeline plots in R to facilitate the comparison of trait value distributions (Wilke, 2018).

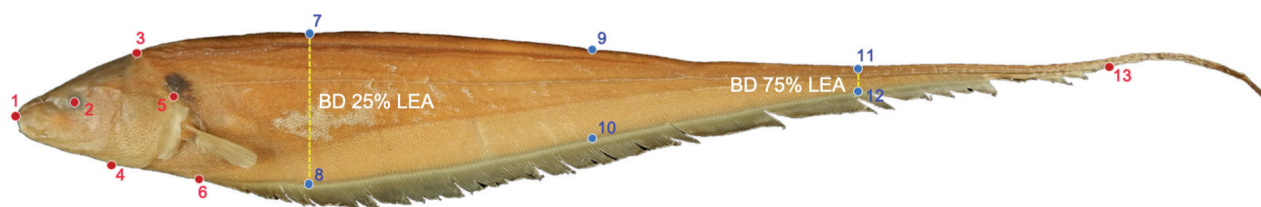


FIGURE 2 | Landmark scheme used in geometric morphometric analyses. Landmarks indicated by small red circles, pseudolandmarks by small blue circles. Landmarks described in Tab. 2. Body depth (BD) measured at 25% and 75% LEA to calculate Taper Ratio (TR). Photograph of *S. macrurus*, ANSP 209719.

Two-dimensional geometric morphometrics (2D GMM) were used to capture shape variation in the new species described herein and for comparison to congeners. Photographs of 91 specimens were taken using a Nikon Coolpix S9700 digital camera with all specimens in the same position in left lateral view with the dorsum forming a nearly straight line from the nape to the end of the anal fin. Photos were then converted to thin plate spline (.tps) files using tpsUtil (Rohlf, 2008), and seven homologous landmarks and six pseudo-landmarks (Fig. 2; Tab. 2) were placed on each photograph using FIJI (ImageJ) (Schindelin *et al.*, 2012). Landmark coordinates were exported as .txt files and then imported into MorphoJ (Klingenberg, 2011) where a Procrustes superimposition was performed to remove the effects of size and scaling among specimens. A principal components analysis (PCA) was then performed in MorphoJ to identify the primary axes of variance. Data for comparison to the new species were collected from an additional 226 specimens from 116 lots of *Sternopygus* belonging to nine other species. These are listed in Tab. 3. Museum codes and abbreviations follow Sabaj (2020).

TABLE 2 | Description of 13 landmarks used in 2D GMM analysis. Note: 7–12 are pseudo-landmarks.

Landmark	Description
1	Anterior margin of upper jaw at mid-axis of body
2	Center of eye
3	Nape at posterior margin of occipital crest
4	Urogenital pore
5	Posterior margin of bony opercle
6	Insertion of anal fin
7	Center of dorsum at 25% LEA
8	Ventral extent of pterygiophores at 25% LEA
9	Center of dorsum at 50% LEA
10	Ventral extent of pterygiophores at 50% LEA
11	Center of dorsum at 75% LEA
12	Ventral extent of pterygiophores at 75% LEA
13	End of anal fin

RESULTS

Sternopygus sarae, new species

urn:lsid:zoobank.org:act:3A5CDAFE-FFA7-4F03-89DA-C5E2E79A12B3

(Figs. 3–13; Tab. 4)

Sternopygus astrabes. —Mago-Leccia, 1994:79–80, 183 (designation of two paratypes in lot AMNH 58643 whose morphometric and meristic values fall outside the current diagnosis for *S. astrabes*).

Sternopygus sp. 'cau'. —Hulen *et al.*, 2005:409–412, 416–426 (original mention). —Santos-Silva *et al.*, 2008:1252, tab. 1 (mention).

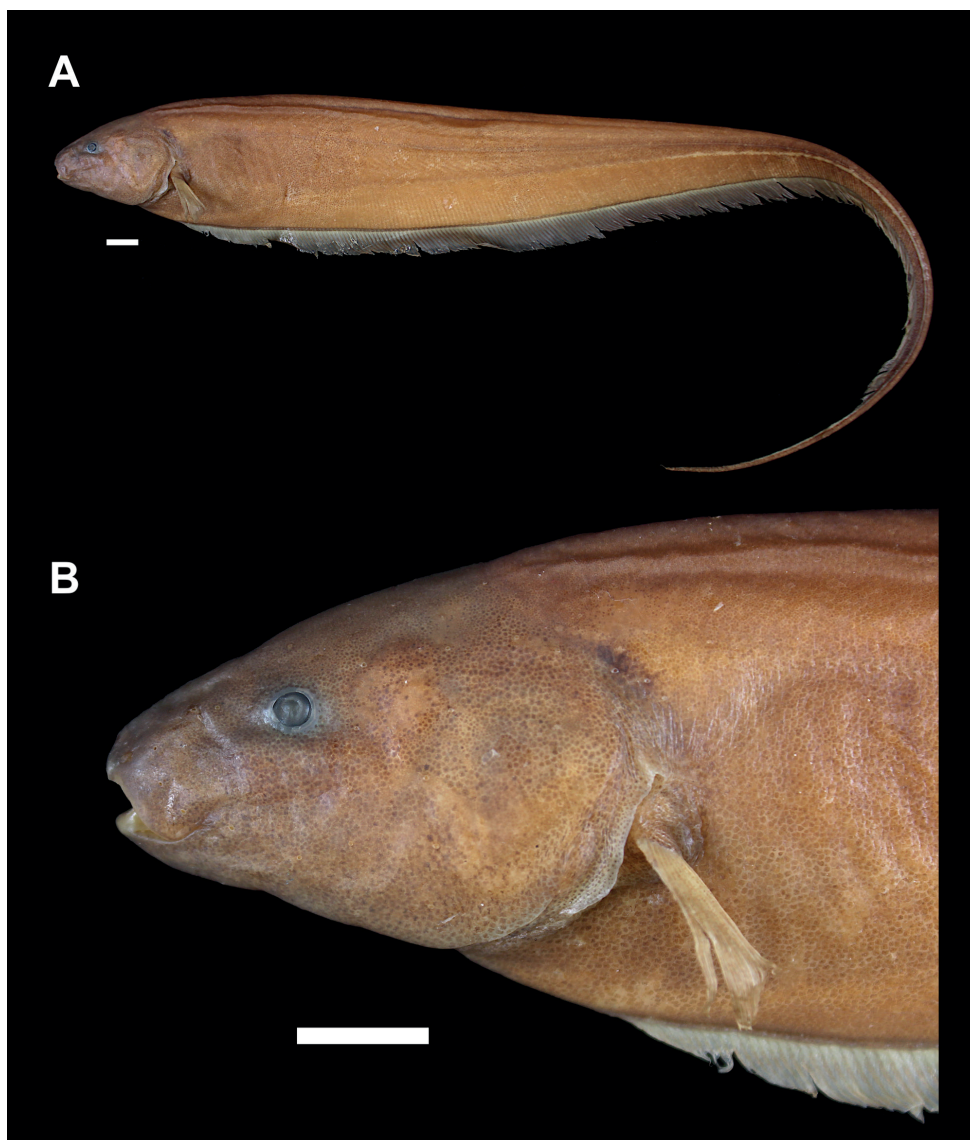


FIGURE 3 | *Sternopygus sarae*, holotype, ANSP 209718, male, 407 mm TL. **A.** Full body; **B.** Closeup of head. Scale bar = 1 cm.

Holotype. ANSP 209718, 407 mm TL (340 mm LEA), male, Venezuela, Bolívar, Río Orinoco basin, confluence of Orinoco and Caura (Las Piedras) rivers, 07°38'36"N 64°50'00"W, 20 Nov 1985, W. Saul, R. Royero, & L. Aguana.

Paratypes. All from Venezuela, Bolívar state, Orinoco basin. AMNH 58643, 2, 261–262 mm TL, creek tributary of Caura River near confluence of Orinoco River, approx. 07°36'N 64°55'W, 22 Nov 1985, B. Chernoff. ANSP 163043, 7, 161–302 mm TL, creek (possibly Caño Curimo) feeding Caura River near confluence of Caura and Orinoco rivers, 07°37'48"N 64°50'42"W, 22 Nov 1985, B. Chernoff, W. Saul, & R. Royero. ANSP 160357, 27, 171–392 mm TL, collected with holotype. MCP 15339, 8, 279–309 mm TL, collected with holotype.

Non-type. AUM 53682, 1, 267 mm TL, Venezuela, Bolívar, Orinoco basin, Orinoco River at Caicara City, 07°38'44.5"N 66°10'46.3"W, 23 Apr 2010, N. K. Lujan, J. Birindelli & V. Meza.

Diagnosis. *Sternopygus sarae* can be distinguished from all other congeners by the presence of three broad, dark vertical pigment bars with irregular margins that extend across the mid-dorsum to the ventral margin of the pterygiophores on the lateral body surfaces (*vs.* no pigment bars in the *S. aequilabiatum* (Humboldt, 1805) group, *S. arenatus* (Eydoux & Souleyet, 1850), *S. branco* Crampton, Hulen & Albert, 2004, *S. macrurus*, and *S. xingu* Albert & Fink, 1996; pigment saddles that do not extend to the base of the pterygiophores in *S. astrabes*, juvenile *S. obtusirostris*, and juvenile *S. sabaji*, and no bars or saddles in adult *S. obtusirostris* and *S. sabaji*; Fig. 1). See Discussion for comments on the appearance and regularity of the pigment bars. *Sternopygus sarae* further differs from all other congeners by a unique combination of characters of head and body proportions, and osteological traits. *Sternopygus sarae* differs from species of the *S. aequilabiatum* group, and from *S. arenatus*, *S. macrurus*, *S. sabaji*, and *S. xingu* in a relatively shorter head length (HL% 9.9–12.2 *vs.* 12.5–19.6), from members of the *S. aequilabiatum* group, *S. branco*, *S. sabaji*, and *S. xingu* in a relatively greater interorbital distance (IO% 27.5–37.6 *vs.* 14.4–26.5), and from *S. arenatus* and *S. branco* in a relatively greater mouth width (MW% 16.0–19.1 *vs.* 11.0–13.9). *Sternopygus sarae* has a proportionally shorter head and more slender body than sympatric congeners (*S. astrabes* and *S. macrurus*). Comparisons of relative head length (HL%) between *S. sarae*, *S. astrabes*, and *S. macrurus* are presented in Fig. 4. HL% values overlap slightly between *S. sarae* and its sympatric congener, *S. astrabes*. *Sternopygus sarae* also has a more slender body shape in lateral profile (BD%) than its sympatric congeners (*S. astrabes* and *S. macrurus*) with overlap only in extreme values (Fig. 4). While not diagnostic, the relatively shorter HL% and BD% of *S. sarae* are still useful in separating most adult specimens from *S. astrabes* and *S. macrurus*.

Sternopygus sarae is most similar to *S. obtusirostris* from the Amazon from which it differs by a lighter body coloration (lateral surfaces pale brown *vs.* dark brown), a lighter coloration of pectoral and anal fin membranes (hyalin *vs.* dark brown), a less tapered body shape in lateral profile (TR% 19.1–21.4 *vs.* 24.6–25.0; Tab. 5), and a less robustly ossified neurocranium with absence of paired ventral ridges of the posterior portion of the parasphenoid anterior limb (*vs.* present; Fig. 5). *Sternopygus sarae* further differs from the partially sympatric *S. astrabes* by having a relatively smaller eye diameter (ED% 6.7–

TABLE 3 | Summary of morphometric and meristic data for all valid species of the genus *Sternopygus*. Measurements reported in millimeters for LEA, AFL, and HL. Abbreviations given in Material and Methods.

Species	LEA			AFL			CA %		
	n	range	mean	n	range	mean	n	range	mean
<i>Sternopygus sarae</i>	40	166–340	219	40	145–303	192	40	8.5–45.7	27.9
<i>Sternopygus aequilabiatu</i> s group	16	160–390	228	16	134–335	189	12	11.0–29.0	17.8
<i>Sternopygus arenatus</i>	6	195–455	329	6	153–380	261	4	10.9–23.1	17.1
<i>Sternopygus astrabes</i>	22	81–177	121	22	64–148	102	16	23.4–43.2	34.0
<i>Sternopygus branco</i>	13	171–353	265	13	141–309	231	13	24.4–41.3	32.9
<i>Sternopygus macrurus</i>	76	140–455	265	66	114–405	224	47	10.6–28.7	18.5
<i>Sternopygus obtusirostris</i>	16	167–520	291	16	120–465	252	10	9.0–25.1	15.7
<i>Sternopygus sabaji</i>	7	130–311	213	7	111–258	179	7	18.9–31.5	25.3
<i>Sternopygus xingu</i>	5	162–446	283	5	134–371	236	3	13.3–27.2	21.0
Species	HL			PO %			PR %		
	n	range	mean	n	range	mean	n	range	mean
<i>Sternopygus sarae</i>	45	19.6–36.5	23.8	45	54.8–63.5	57.4	45	33.2–39.9	35.9
<i>Sternopygus aequilabiatu</i> s group	16	23.5–55.8	34.2	16	55.9–60.0	58.7	16	30.6–36.0	33.1
<i>Sternopygus arenatus</i>	6	32.7–62.2	47.5	6	56.3–59.1	57.6	6	32.7–37.5	35.2
<i>Sternopygus astrabes</i>	22	11.2–23.4	16.0	22	48.2–59.5	54.2	22	28.9–35.5	32.7
<i>Sternopygus branco</i>	13	24.4–41.3	32.9	13	50.8–54.9	53.0	13	36.1–40.6	38.4
<i>Sternopygus macrurus</i>	66	18.2–63.0	37.8	66	51.6–60.8	56.5	66	30.8–39.3	36.1
<i>Sternopygus obtusirostris</i>	16	20.1–54.2	33.6	16	53.4–61.2	57.3	16	31.0–35.9	34.0
<i>Sternopygus sabaji</i>	7	19.9–48.2	30.3	7	55.2–57.0	56.1	7	34.5–37.1	36.0
<i>Sternopygus xingu</i>	5	26.3–75.6	49.3	5	54.7–59.3	56.7	5	31.9–33.9	33.0
Species	MW %			BO %			HD %		
	n	range	mean	n	range	mean	n	range	mean
<i>Sternopygus sarae</i>	37	16.0–19.1	17.6	36	25.0–36.3	30.7	45	58.9–79.4	70.9
<i>Sternopygus aequilabiatu</i> s group	16	11.1–16.8	13.2	16	20.0–27.8	23.8	16	59.5–67.7	62.0
<i>Sternopygus arenatus</i>	2	11.0–13.8	12.4	2	15.7–16.5	16.1	2	68.8–73.4	71.1
<i>Sternopygus astrabes</i>	22	12.8–20.9	15.5	22	28.9–48.0	37.1	22	66.4–77.4	72.3
<i>Sternopygus branco</i>	13	12.3–13.9	12.9	13	25.9–31.1	28.2	13	57.8–68.4	64.7
<i>Sternopygus macrurus</i>	66	13.4–21.4	16.8	66	25.4–50.0	31.3	66	64.8–80.2	71.3
<i>Sternopygus obtusirostris</i>	16	14.4–17.6	15.8	16	25.4–45.3	36.9	16	68.6–79.5	73.8
<i>Sternopygus sabaji</i>	7	19.4–23.4	20.8	7	27.0–31.9	29.7	7	60.7–74.6	70.3
<i>Sternopygus xingu</i>	5	17.1–19.8	18.5	5	35.2–51.4	42.1	5	65.3–75.7	69.1
Species	PCV			P1R			AFR		
	n	range	median	n	range	median	n	range	median
<i>Sternopygus sarae</i>	10	24–26	24	44	14–16	15	41	278–325	302
<i>Sternopygus aequilabiatu</i> s group	16	23–25	24	20	14–17	17	16	228–310	284
<i>Sternopygus arenatus</i>	6	21–24	21	9	15–17	15	1	215–215	215
<i>Sternopygus astrabes</i>	29	18–19	19	23	15–17	16	19	170–298	200
<i>Sternopygus branco</i>	12	25–27	26	13	12–15	13	12	250–340	278
<i>Sternopygus macrurus</i>	52	24–28	26	95	13–17	15	44	195–300	256
<i>Sternopygus obtusirostris</i>	14	22–26	25	20	15–15	15	14	195–312	285
<i>Sternopygus sabaji</i>	5	21–22	22	18	15–15	15	18	204–237	220
<i>Sternopygus xingu</i>	4	28–29	29	6	12–15	12	4	292–321	312



TABLE 3 | (Continued)

Species	BD %			BW %			HL %		
	n	range	mean	n	range	mean	n	range	mean
<i>Sternopygus sarae</i>	41	8.8–10.7	9.9	41	3.9–5.4	4.7	41	9.9–12.2	10.9
<i>Sternopygus aequilabiatu</i> s group	16	10.5–13.8	12.1	16	5.3–6.3	5.9	16	13.4–16.1	15.1
<i>Sternopygus arenatus</i>	2	12.4–13.3	12.9	2	5.8–5.9	5.9	6	13.2–16.8	14.6
<i>Sternopygus astrabes</i>	22	10.4–12.4	11.5	22	4.6–6.6	5.5	22	11.7–14.7	13.3
<i>Sternopygus branco</i>	13	8.3–10.9	9.3	13	4.2–6.4	4.5	13	11.4–14.3	12.6
<i>Sternopygus macrurus</i>	66	10.3–15.2	12.8	66	4.8–8.3	6.1	66	12.5–16.8	14.3
<i>Sternopygus obtusirostris</i>	16	9.5–12.2	10.6	16	3.9–6.0	4.7	16	10.4–12.7	11.7
<i>Sternopygus sabaji</i>	7	12.1–14.3	12.7	7	5.4–7.0	6.1	7	14.3–15.5	15.0
<i>Sternopygus xingu</i>	5	13.4–16.1	14.4	5	6.2–8.2	6.8	5	16.2–19.6	17.2
Species	ED %			IO %			NN %		
	n	range	mean	n	range	mean	n	range	mean
<i>Sternopygus sarae</i>	45	6.7–10.6	8.3	45	27.5–37.6	30.5	45	12.7–18.0	16.1
<i>Sternopygus aequilabiatu</i> s group	16	6.8–9.8	8.6	16	14.4–21.7	17.5	16	10.2–14.4	12.2
<i>Sternopygus arenatus</i>	2	7.4–9.8	8.6	2	22.4–33.0	27.7	2	7.4–9.8	8.6
<i>Sternopygus astrabes</i>	22	13.8–19.5	15.5	22	23.8–30.4	26.1	17	14.5–19.8	17.3
<i>Sternopygus branco</i>	13	9.8–13.5	10.7	13	22.2–25.7	24.2	13	14.9–17.4	16.0
<i>Sternopygus macrurus</i>	66	7.5–14.6	10.3	66	17.6–31.7	25.5	66	8.3–17.9	13.9
<i>Sternopygus obtusirostris</i>	16	10.1–13.5	11.9	16	22.7–28.3	24.9	16	13.5–20.0	16.9
<i>Sternopygus sabaji</i>	7	7.6–9.3	8.2	7	23.6–26.5	25.3	7	14.5–16.4	15.0
<i>Sternopygus xingu</i>	5	6.7–12.2	9.4	5	16.7–22.4	24.8	5	11.4–15.6	13.3
Species	HW %			PA %			P1 %		
	n	range	mean	n	range	mean	n	range	mean
<i>Sternopygus sarae</i>	45	36.9–53.2	45.9	45	32.2–67.6	42.4	45	43.6–57.8	50.6
<i>Sternopygus aequilabiatu</i> s group	16	35.9–44.6	38.8	16	40.1–56.3	47.0	16	43.7–53.3	48.8
<i>Sternopygus arenatus</i>	2	42.8–47.1	44.9	2	61.6–67.0	64.3	6	40.0–56.0	45.0
<i>Sternopygus astrabes</i>	22	37.5–51.9	46.4	22	14.3–52.6	39.4	22	43.6–67.8	58.0
<i>Sternopygus branco</i>	13	36.1–43.4	39.8	13	30.3–38.2	33.8	13	50.0–57.2	53.2
<i>Sternopygus macrurus</i>	66	33.5–59.4	46.7	66	32.7–65.1	47.6	64	37.8–64.7	48.6
<i>Sternopygus obtusirostris</i>	16	36.7–50.7	42.9	16	29.0–50.9	37.1	16	45.8–60.5	52.3
<i>Sternopygus sabaji</i>	7	39.9–47.8	43.5	7	29.9–53.2	41.2	7	44.1–52.4	47.6
<i>Sternopygus xingu</i>	5	38.8–47.3	43.4	5	32.7–42.4	36.6	5	36.8–43.0	39.7
Species	SAL			SBL			SOP		
	n	range	median	n	range	median	n	range	median
<i>Sternopygus sarae</i>	7	15–20	18	7	9–13	11	7	19–22	20
<i>Sternopygus aequilabiatu</i> s group	18	12–24	17	18	7–13	9	18	10–16	13
<i>Sternopygus arenatus</i>	6	15–16	16	6	7–9	8	6	15–16	16
<i>Sternopygus astrabes</i>	19	11–18	15	19	9–14	12	19	10–16	14
<i>Sternopygus branco</i>	10	17–26	19	10	13–17	16	10	13–20	17
<i>Sternopygus macrurus</i>	55	12–22	16	55	6–20	9	55	9–15	13
<i>Sternopygus obtusirostris</i>	18	15–21	18	18	7–13	11	18	14–19	17
<i>Sternopygus sabaji</i>	5	12–14	13	5	5–5	5	5	12–15	13
<i>Sternopygus xingu</i>	3	14–16	15	3	6–8	7	3	14–19	18

TABLE 4 | Absolute values of morphometric and meristic data for specimens of the type series of *Sternopygus sarae*. Abbreviations defined in Material and Methods.

	Holotype	Min	Max	Mean	Median	N
TL	407	216	407	280	–	40
LEA	340	166	340	219	–	41
AFL	303	145	303	192.7	–	41
CA	68	17	86	60.6	–	40
BD	35.0	16.9	35.0	21.5	–	45
BW	18.5	7.1	18.5	10.2	–	45
HL	36.5	19.6	36.5	23.8	–	45
PO	21.2	11.4	21.2	13.7	–	45
PR	13.4	7.0	13.4	8.5	–	45
ED	2.7	1.6	2.7	2.0	–	45
IO	10.8	5.5	10.8	7.2	–	45
NN	5.7	3.1	5.7	3.8	–	45
MW	6.7	3.3	6.7	4.3	–	45
BO	11.4	4.9	11.4	7.4	–	36
HD	27.8	13.5	27.8	16.9	–	45
HW	19.4	7.7	19.4	11.0	–	45
PA	16.8	6.4	16.8	10.1	–	45
P1	16.5	9.3	16.5	12.0	–	45
PCV	24	24	26	–	24	10
P1R	15	14	16	–	15	44
AFR	308	278	325	–	302	41
SAL	20	15	20	–	18	7
SBL	13	9	13	–	11	7
SOP	19	19	22	–	20	7

10.6 vs 13.8–19.5), a greater taper ratio (TR% 19.1–21.4 vs. 15.2–18.5), more precaudal vertebrae (PCV 24–26 vs. 18–19), and the lack of paired ventral ridges of the posterior portion of the parasphenoid anterior limb (vs. present). *Sternopygus sarae* can be further distinguished from *S. sabaji* by 11 pores in the preopercular-mandibular laterosensory line (vs. 10), presence of conical teeth on the ventral surface of the endopterygoid (vs. no teeth), more precaudal vertebrae (PCV 24–26 vs. 21–22), more anal-fin rays (AFR 278–325 vs. 204–237), and more scales above the lateral line (SAL 16–17 vs. 12–14). *Sternopygus sarae* also differs from *S. xingu* by fewer precaudal vertebrae (PCV 24–26 vs. 28–29). Morphometric and meristic comparisons among *Sternopygus* species are provided in Tab. 3. The new species readily differs from another barred sternopygid, *Japigny kirschbaum* Meunier, Jégu & Keith, 2011 from the Atlantic coast basins of the Guiana Shield, by the possession of all unbranched anal-fin rays and a free orbital margin.

TABLE 5 | Taper Ratio (TR) values for 25 specimens representing four species of *Sternopygus*. Abbreviations defined in Material and Methods.

Species	Lot	LEA	TR
<i>S. astrabes</i>	ANSP 162663	138	15.2%
<i>S. astrabes</i>	ANSP 162663	178	18.5%
<i>S. astrabes</i>	INHS 61503	106	16.8%
<i>S. astrabes</i>	INHS 61503	113	17.5%
<i>S. astrabes</i>	INHS 61503	121	17.1%
<i>S. astrabes</i>	INHS 61503	129	16.8%
<i>S. astrabes</i>	INHS 61503	138	15.8%
<i>S. astrabes</i>	INHS 61503	144	15.8%
<i>S. astrabes</i>	INHS 61503	155	16.1%
<i>S. astrabes</i>	INHS 61503	188	15.7%
<i>S. macrurus</i>	UF 80276	239	24.2%
<i>S. macrurus</i>	UF 80276	170	21.7%
<i>S. macrurus</i>	UF 80276	161	18.5%
<i>S. obtusirostris</i>	INPA 6430	508	25.0%
<i>S. obtusirostris</i>	MCP 32262	490	24.6%
<i>S. sarae</i>	ANSP 160357	187	20.3%
<i>S. sarae</i>	ANSP 160357	195	21.4%
<i>S. sarae</i>	ANSP 160357	208	20.4%
<i>S. sarae</i>	ANSP 160357	209	21.2%
<i>S. sarae</i>	ANSP 160357	225	20.2%
<i>S. sarae</i>	ANSP 160357	231	19.8%
<i>S. sarae</i>	ANSP 160357	235	20.8%
<i>S. sarae</i>	ANSP 160357	272	19.1%
<i>S. sarae</i>	ANSP 160357	310	20.0%
<i>S. sarae</i>	ANSP 209718	340	20.4%

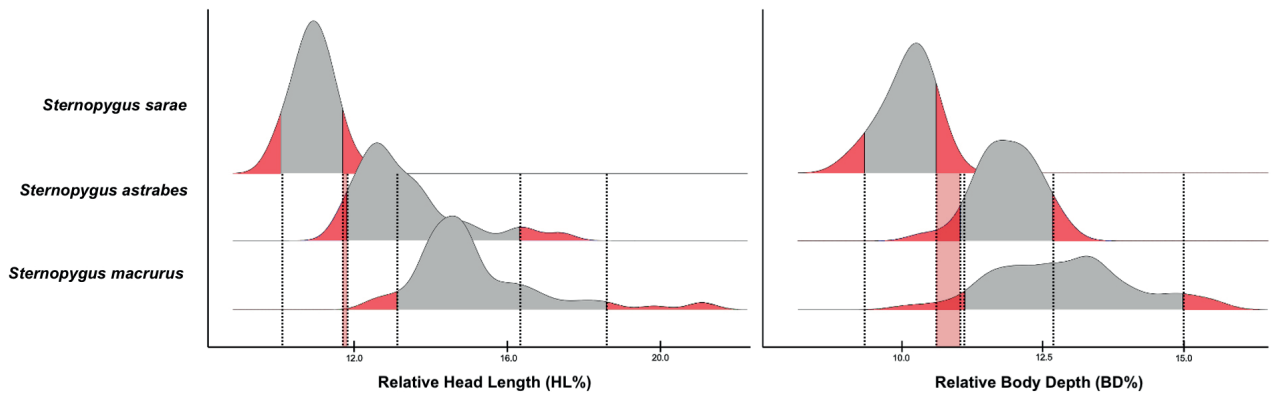


FIGURE 4 | Ridgeline plots of relative head length (HL%) and relative body depth (BD%) as a percentage of LEA for three sympatric *Sternopygus* species in the Guiana Shield region. Dark red regions indicate values outside 95% confidence interval from the mean; light red indicates overlapping values outside the 95% confidence interval.

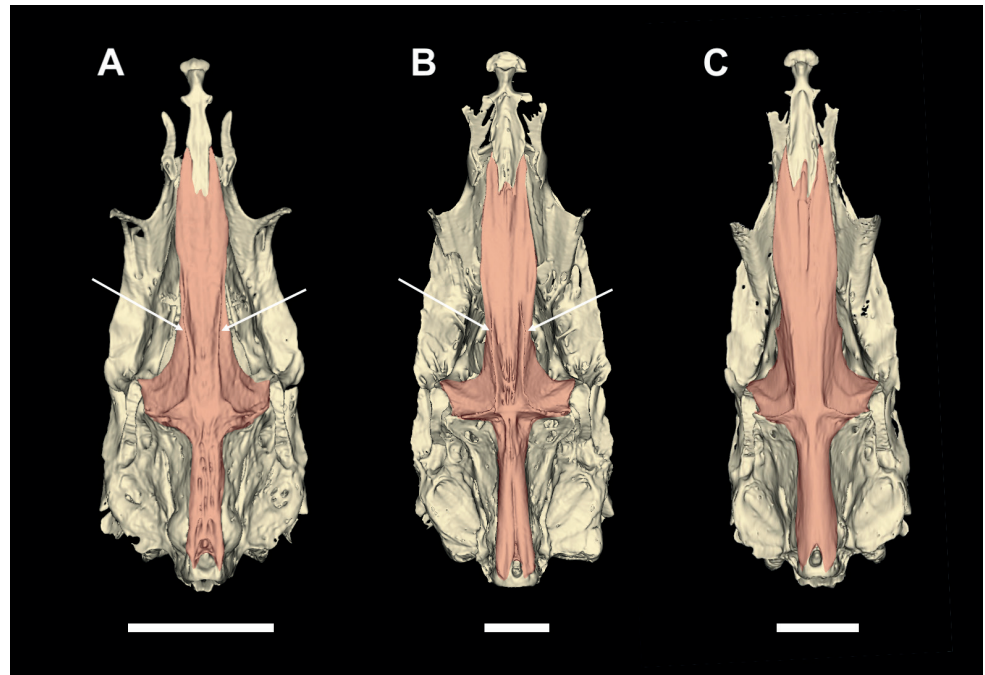


FIGURE 5 | Micro-CT renderings of the ventral surface of the neurocrania of three species of *Sternopygus* with the endopterygoid highlighted in red. **A.** *Sternopygus astrabes*, INHS 61503; **B.** *Sternopygus obtusirostris*, INPA 6430; **C.** *Sternopygus sarae*, ANSP 209718. Arrows indicate ridges along ventral surface of endopterygoid in *S. astrabes* and *S. obtusirostris*, which are not present in *S. sarae*. Note: the presence of the ridges is not a function of body size. Scale bars = 5 mm.

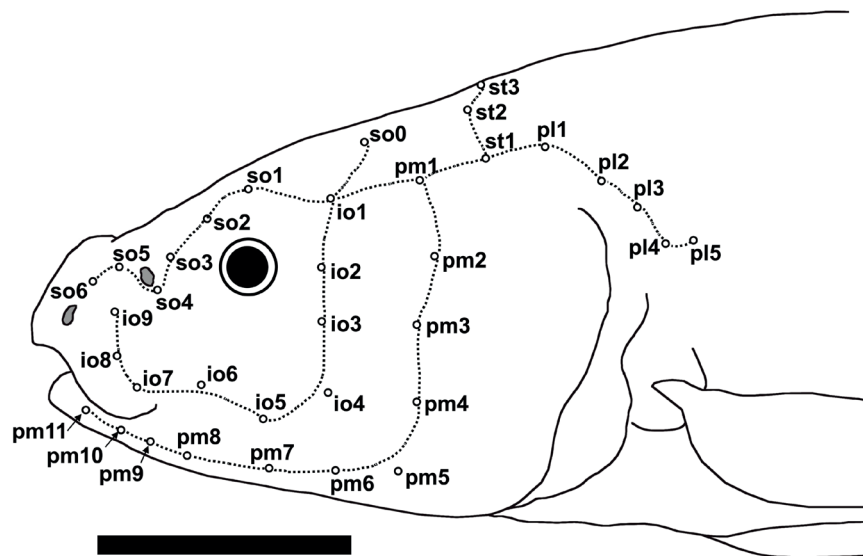


FIGURE 6 | Diagram of cephalic sensory canal pore configuration of the head in left lateral view of *Sternopygus sarae*, ANSP 160357, paratype, 274 mm TL. Lateral sensory pores indicated by circles. Centerline of canals estimated by dashed lines. Anterior and posterior nares shaded gray. Supraorbital (so), infraorbital (io), posterior (pl), preopercular-mandibular (pm), and supratemporal (st) laterosensory canals. so0 indicates the otic canal. Scale bar = 1 cm.

Description. Head and body shape in Fig. 3; cephalic mechanosensory line and pore configuration in Fig. 6; morphometric and meristic data in Tab. 4; and body size distribution of type series in Fig. 7. Maximum known body size 407 mm TL (340 mm LEA). Body elongate and slender compared to sympatric congeners, *S. astrabes* and *S. macrurus* (Fig. 8), somewhat compressed laterally in body cavity region, more laterally compressed in post-coelomic body region; body widest immediately behind head; whole body covered in ovoid (axially elongate) cycloid scales, except head and fins. Lateral line complete and non-interrupted, extending onto tail posterior to last anal-fin ray. Longitudinal stripe thin and extending along posterior half of body, sometimes very faint or absent. Eyes relatively small, and not covered by layer of skin. Body relatively shallow with short head length relative to most congeners. Anterior naris slightly tubular, posterior naris non-tubular. 14–16 total pectoral-fin rays. 278–325 anal-fin rays, all unbranched. 24–26 precaudal vertebrae. Pigment pattern composed of three alternating dark bars. Bars (B1–B3) composed of less densely arranged chromatophores with larger diameters. Interbars (I1, I2) composed of more densely arranged chromatophores with smaller diameters (Fig. 9).

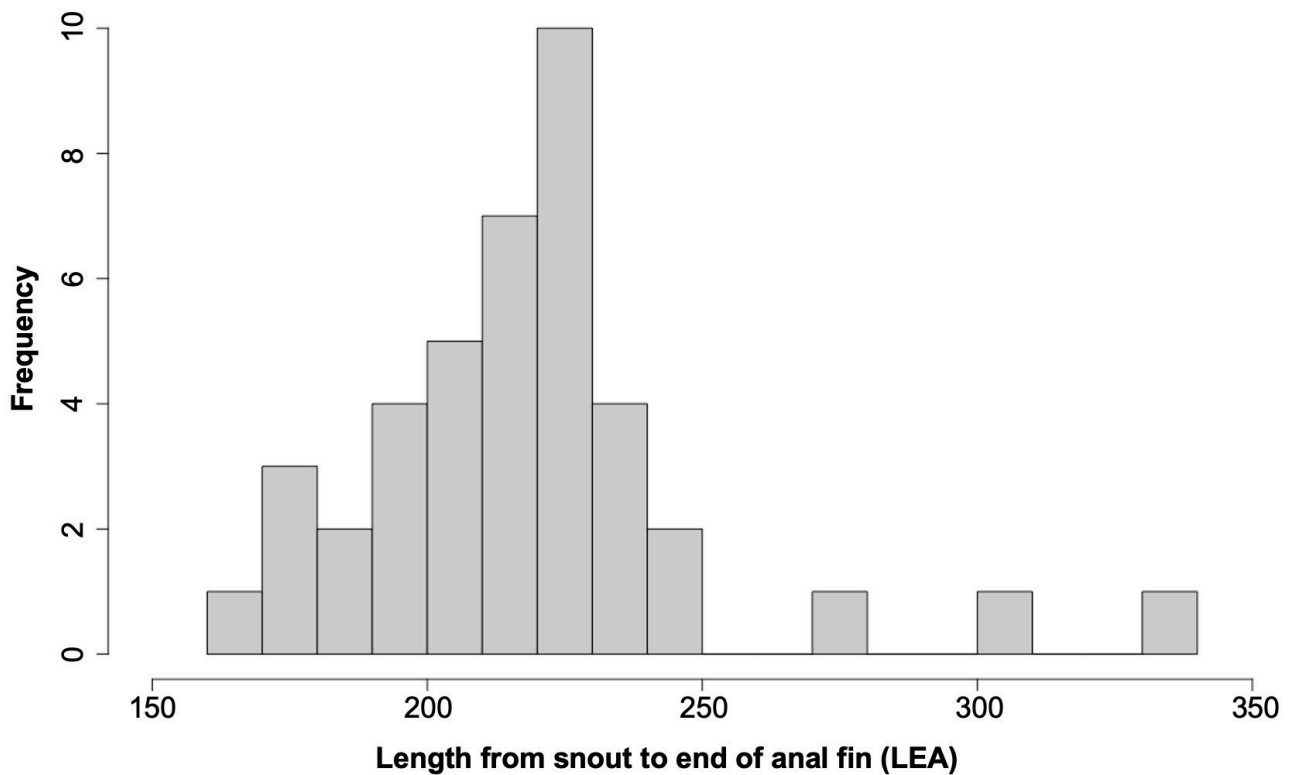


FIGURE 7 | Histogram of specimen sizes, reported in LEA, of all 46 specimens comprising the type series of *Sternopygus sarae*.



FIGURE 8 | Full body photographs of three valid and sympatric species of *Sternopygus* from the Orinoco River drainage **A.** *Sternopygus macrurus*, ANSP 209719 (192 mm TL); **B.** *Sternopygus sarae*, ANSP 160357 (216 mm TL); **C.** *Sternopygus astrabes*, INHS 61503 (228 mm TL). Scale bars = 1 cm.

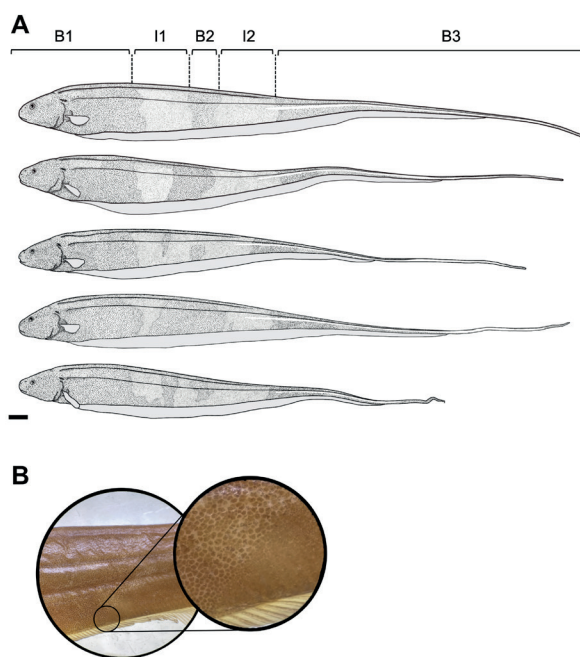


FIGURE 9 | **A.** Line drawing of five paratype specimens of *Sternopygus sarae* (ANSP 160357). Top two drawings depict typical coloration pattern, lower three drawings depict uncommon variations of pigmentation seen in preserved specimens. Scale bar = 1 cm. Bars (B1–B3) are composed of less densely arranged chromatophores that have larger diameters. Interbars (I1, I2) are composed of more densely arranged chromatophores that have smaller diameters. Homologous chromatophore fields with barred and interbarred regions are labeled for all four of the barred *Sternopygus* species. **B.** Close-up of specimen showing differences of size and density of chromatophores making up the bar and interbar regions. Note: bar appearance differs when viewed at whole body vs close-up such that pigment patches with large chromatophores and large inter-chromatophore spaces appear darker when specimen is viewed as a whole (*e.g.*, at arms distance, panel **A** as compared to lighter when viewed close up panel **B**).

Neurocranium. Neurocranium in dorsal, lateral, and ventral views in Fig. 10. Preorbital region of neurocranium rounded and slightly decurved in lateral view, dorsal margin convex along its entire extent from tip of mesethmoid to posterior margin of parietal, parasphenoid ventral margin slightly concave in lateral view anterior to basiptyergoid process (*sensu* Arratia, 2013: fig. 48), or parasphenoid lateral wing (*sensu* Adriaens, Verraes, 1998: fig. 19b). Neurocranium relatively well-ossified compared to other gymnotiforms, all bones of braincase ossified to their peripheral margins with little or no intervening cartilaginous plates. Supraorbital canal mostly fused to frontal. Lateral ethmoid cartilage well ossified, its ventral margin extending lateral to vomer. Sphenotic small, lateral process not extending beyond lateral neurocranium margin. Foramen between parasphenoid, pterosphenoid, and orbitosphenoid relatively small, bones of ethmoid region (*e.g.*, lateral ethmoid, ventral ethmoid) relatively well-ossified as compared to congeners. Anterior and posterior cranial fontanelles large, separated by narrow interorbital bridge, posterior fontanelle extending posterior to about vertical with anterior margin of exoccipital. Antorbital and postorbital processes of frontal robust, anterior process tapering to distal tip. Parasphenoid anterior portion wider than posterior portion; parasphenoid ventral margin flat, without longitudinal ridges on lateral margins, but with pronounced transversely oriented basiptyergoid ridges.

Oral jaws. Mouth terminal to slightly inferior, anterior margin of mesethmoid extending slightly anterior to anterior margin of dentary; Premaxilla ovoid in frontal view with five unevenly arranged tooth rows on each side, with nine large straight conical teeth on posterior margin, and approximately 35 large, straight conical teeth in anterior four rows. Maxilla broad, with pronounced lateral ridge, and angled at two thirds distance of posterior blade. Dentary of intermediate length, oral margin about as long distance from mandibular symphysis to dentary-retroarticular articulation. Dentary dentition “brush-shaped” (*sensu* Mago-Leccia, 1978), with approximately 85 mostly recurved teeth arranged in 4–5 irregular rows near mental symphysis tapering laterally to single tooth at posterolateral margin of tooth field. Dentary anteroventral margin without small ventral process. Anterior portion of preoperculo-mandibular laterosensory canal completely ossified on medial margin with three constrictions along lateral margin of dentary descending process.

Suspensorium (Fig. 11). All elements of suspensorium well-ossified. Hyomandibula broad with two large foramina on dorsomedial surface (through which pass nerves V, VII, and lateralis) and four separate foramina on lateral surface (through which pass posterior, supraorbital, infraorbital, and preoperculo-mandibular rami of same nerves); for comparison see Albert *et al.*, 2005: fig. 14. Symplectic incompletely ossified at dorsoposterior margin. Quadrate well-ossified and abutting endopterygoid but with cartilaginous margin with metapterygoid. Metapterygoid lower portion poorly ossified. Endopterygoid broad, with about 16 pointed teeth on anterior margin of medial surface, medial margin not contacting other contralateral endopterygoid at midline of palate, endopterygoid ascending process tapering dorsally, connected by thin tendon to ventral surface of frontal. Ascending process of endopterygoid slightly curved posteromedially. Palatine unossified.

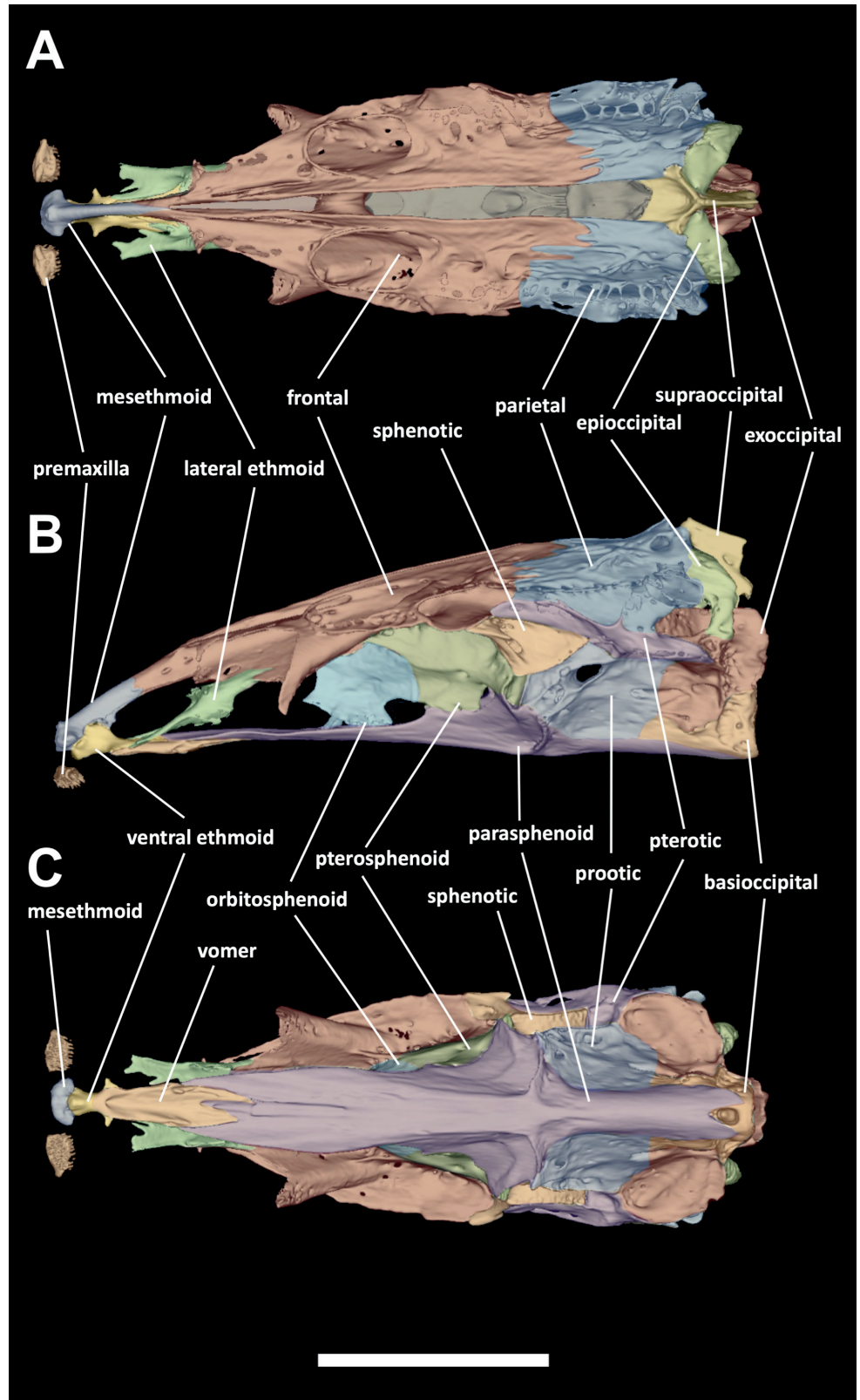


FIGURE 10 | *Sternopygus sarae* neurocranium 3D rendering from micro-CT scan of holotype, ANSP 209718. **A.** Dorsal view; **B.** Lateral view; **C.** Ventral view. The enlarged canal bones fused to the frontal and parietal bones of the neurocranium were included in those segments. Scale bar = 1 cm.

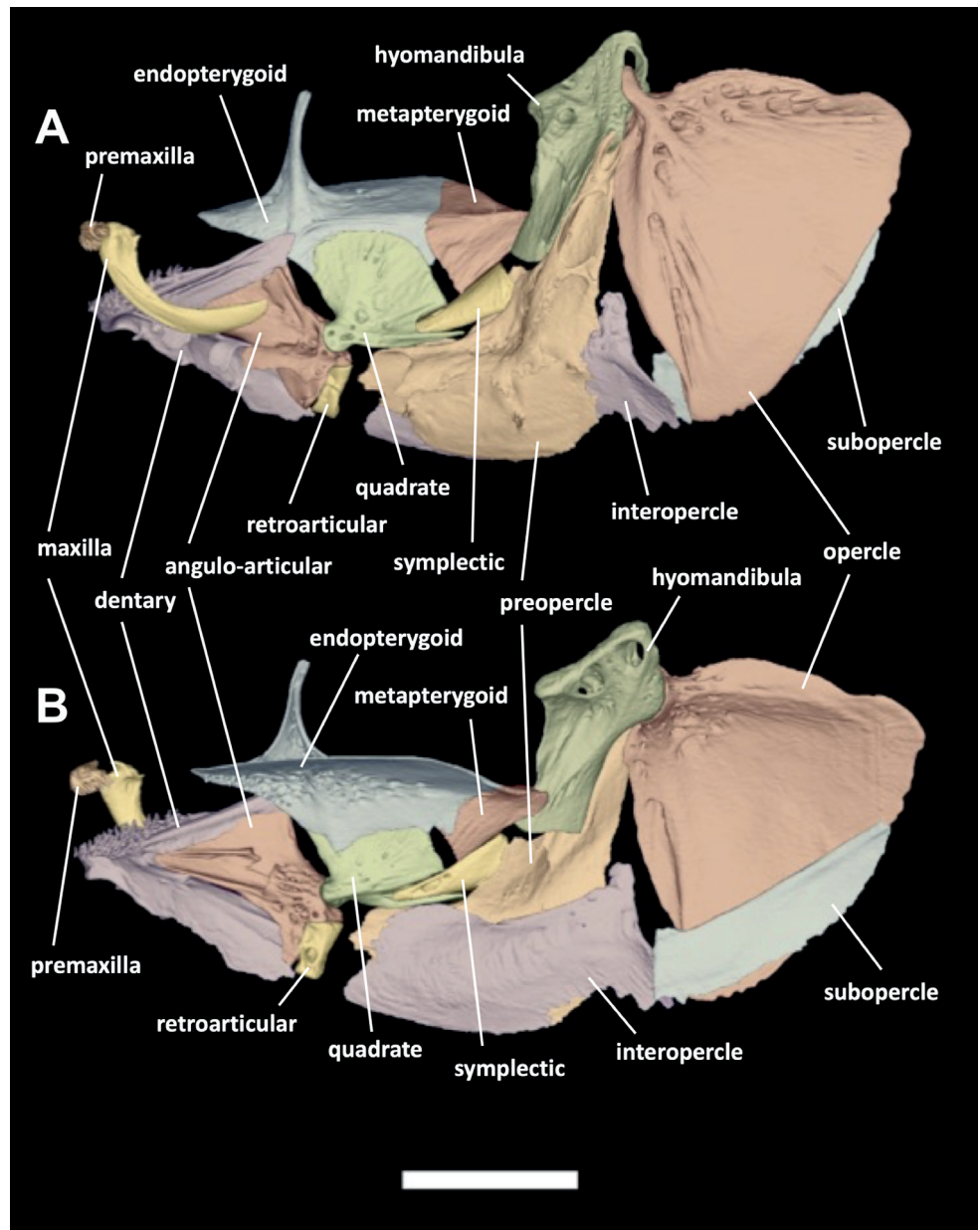


FIGURE 11 | *Sternopygus sarae* suspensorium and opercular series 3D rendering from micro-CT scan of holotype, ANSP 209718. **A.** Lateral view of left side; **B.** Medial view of same side (reversed). Scale bar = 5 mm.

Opercular series (Fig. 11). Opercle well ossified with rounded dorsal, anterior, and posterior margins, dorsal margin with broad median shelf, anterior and posterior margins convex, anterior articulating process large and horn-shaped, lateral opercular surface mostly smooth with large lacunae in ventral and dorsal fields. Preopercle poorly ossified, posterior, ventral, and anterior margins ragged, anterior margin unossified.

Branchial basket. Urohyal well-ossified, posterior blade extending to third branchial arch. Basihyal fan-shaped, basibranchial of third arch cone-shaped, fourth and fifth arches unossified. Hypohyals without medial process and not contacting each other at ventral midline. Five basibranchials, anterior two slender, posterior three broad. Pharyngeal jaws large and robust, pharyngobranchials of fifth branchial arch with 18–20 large conical teeth arranged in 3–4 irregular rows, opposed to large hypobranchials with 9–10 large conical teeth arranged in three irregular rows. Ceratobranchial of fifth arch with large triangular lateral margin. 5–6 squat gill rakers, about as wide as long, in irregular rows on anterodorsal and anteroventral margins of ceratobranchials of all five gill arches.

Pectoral girdle (Fig. 12). Cleithrum well-ossified, anterior portion rounded and broadly contacting contralateral cleithrum at its anterior margin, ascending portion with sharp ridge on anterior margin of lateral surface. Anterior coracoid process thin and elongate, extending halfway to anterior tip of cleithrum. Supracleithrum fused to post temporal. Mesocoracoid unossified. Scapula fused to cleithrum. Five ossified proximal pectoral fin radials, lateral three fused at their bases.

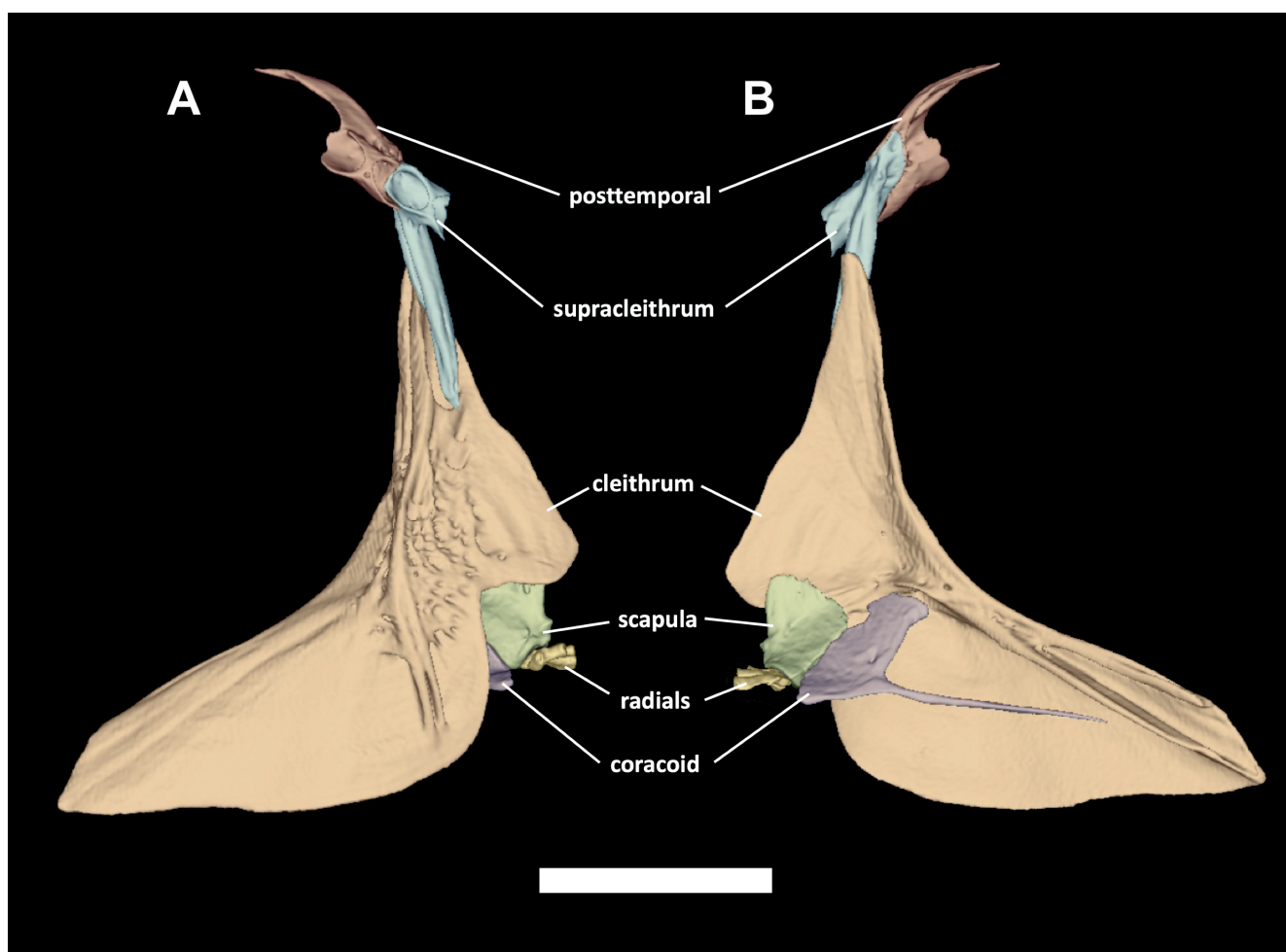


FIGURE 12 | *Sternopygus sarae* pectoral girdle 3D rendering from micro-CT scan of holotype, ANSP 209718. **A.** Lateral view of left side; **B.** Medial view of same side. Scale bar = 5 mm.

Weberian apparatus (Fig. 13). Composed of anterior four vertebrae and their articulating elements. Vertebral centra increasing in size posteriorly, both in diameter and axial extent. V1 being approximately half width and thickness of V4. Parapophysis of V2 (2nd parapophysis) expanded laterally with large facet or hollow on its anterior margin and pointed distal margin (*vs.* truncate with vertical lateral margin in *S. astrabes*). Suspensorium anterior margins well separated, posterior margins meet at point on ventral midline (*vs.* meet with broad symphysis in *S. astrabes*). Intercalarium narrow, less than axial thickness of V1 (*vs.* broader in *S. astrabes* and *S. macrurus* from Amazon basin). Tripus sickle-shaped, its anterior margin broadly contacting intercalarium across its entire extent. Its posterior margin tapering and long and thin (*vs.* short and robust in *S. macrurus*). Lateral process of 4th parapophysis articulating with rib relatively small, anteriorly oriented, about as wide as first vertebral centrum (*vs.* large and posterolaterally oriented in *S. macrurus*). Scaphium large, width approximately 1.5 that of V1 (*vs.* small approximately 1.0 that of V1 in *S. macrurus*, and 1.2 in *S. astrabes*). Supraneural gracile and curved, its dorsal limb oriented vertically (*vs.* robust vertical limb oriented anteriorly in *S. astrabes* and *S. macrurus*). Neural spine of fourth arch tapering distally to acute point (*vs.* truncate in *S. macrurus*).

Color in alcohol. Base color yellow to orange or light brown, without countershading. Two to four broad vertical bars with irregular margins along body extending from dorsomedial margin to anal-fin border. Vertical bars composed of large chromatophores spread at lower density than smaller chromatophores that compose base color. Cream colored longitudinal stripe thin and extending along posterior half of body, sometimes very faint or absent. Anal fin hyaline with dark anal-fin rays. Humeral blotch small, thin, and without well-defined margins (Figs. 3, 8).

Sexual dimorphism. Direct examination of the gonads of six specimens revealed no apparent sexual dimorphism in the proportions of body depth, head length, or any other obvious characters. However, we note that the largest specimens examined (271 mm, 307 mm, 340 mm LEA) were found to be males and the smaller specimens examined were either female or too immature to reliably sex.

Geographical distribution. *Sternopygus sarae* is known from the confluence of Orinoco and Caura rivers (Fig. 14) and from the Orinoco River at Caicara City, Venezuela.

Ecological notes. *Sternopygus sarae* is known from river margins and small channels on the floodplain of a sediment-rich, white water river. Most of the specimens used in this description were collected from near the confluence of the Orinoco and Caura rivers, and a single specimen from Caicara City on the Orinoco River about 150 km upstream from this confluence.

Etymology. We name this species in honor of Dr. Sara Holmberg Albert, for her perennial support to the last author. A noun in the singular genitive case. Popular name: Sara's Longtail Knifefish.

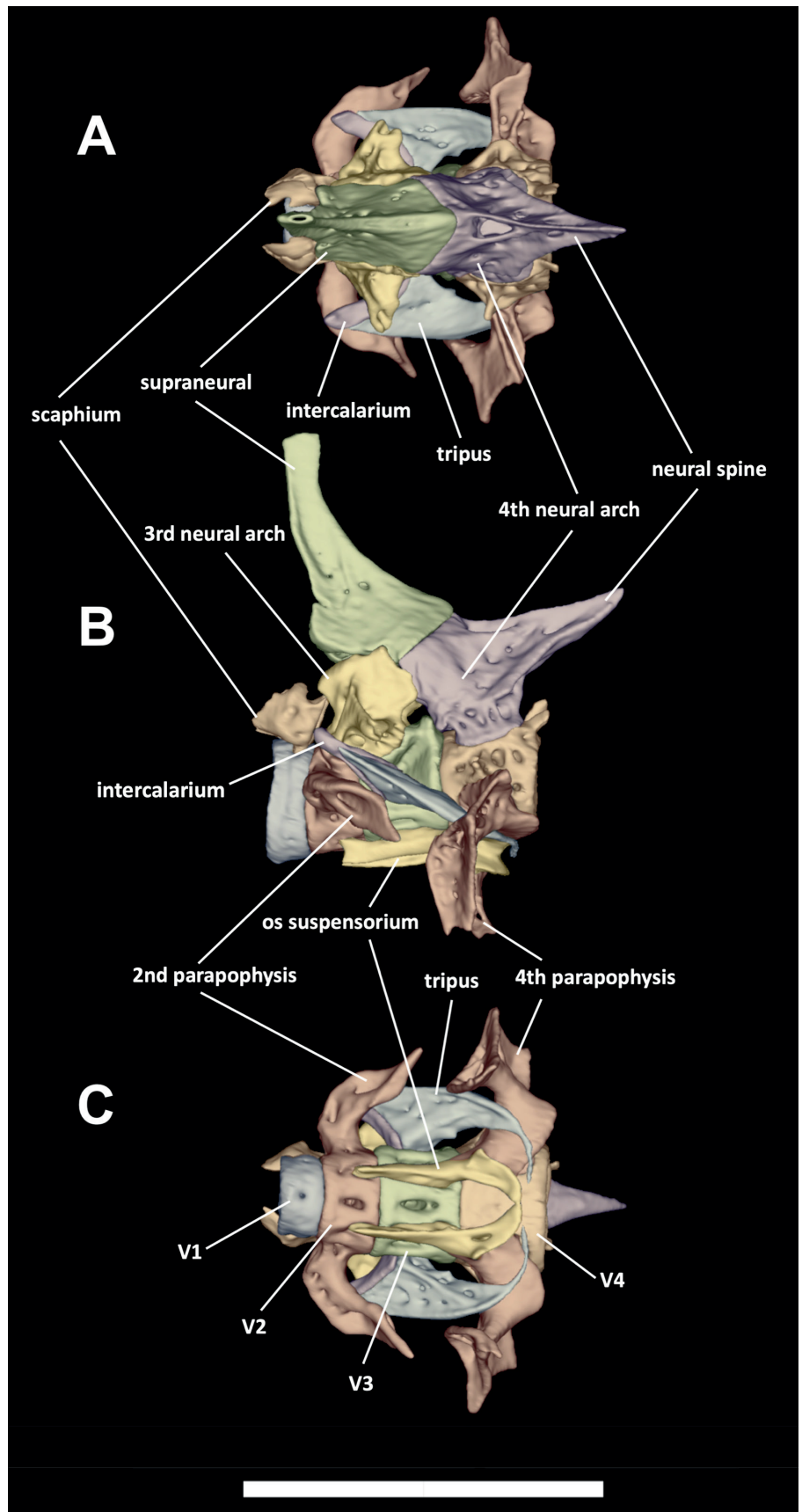


FIGURE 13 | *Sternopygus sarae* Weberian apparatus 3D rendering from micro-CT scan of holotype, ANSP 209718. **A.** Dorsal view; **B.** Lateral view; **C.** Ventral view. Scale bar = 5 mm.

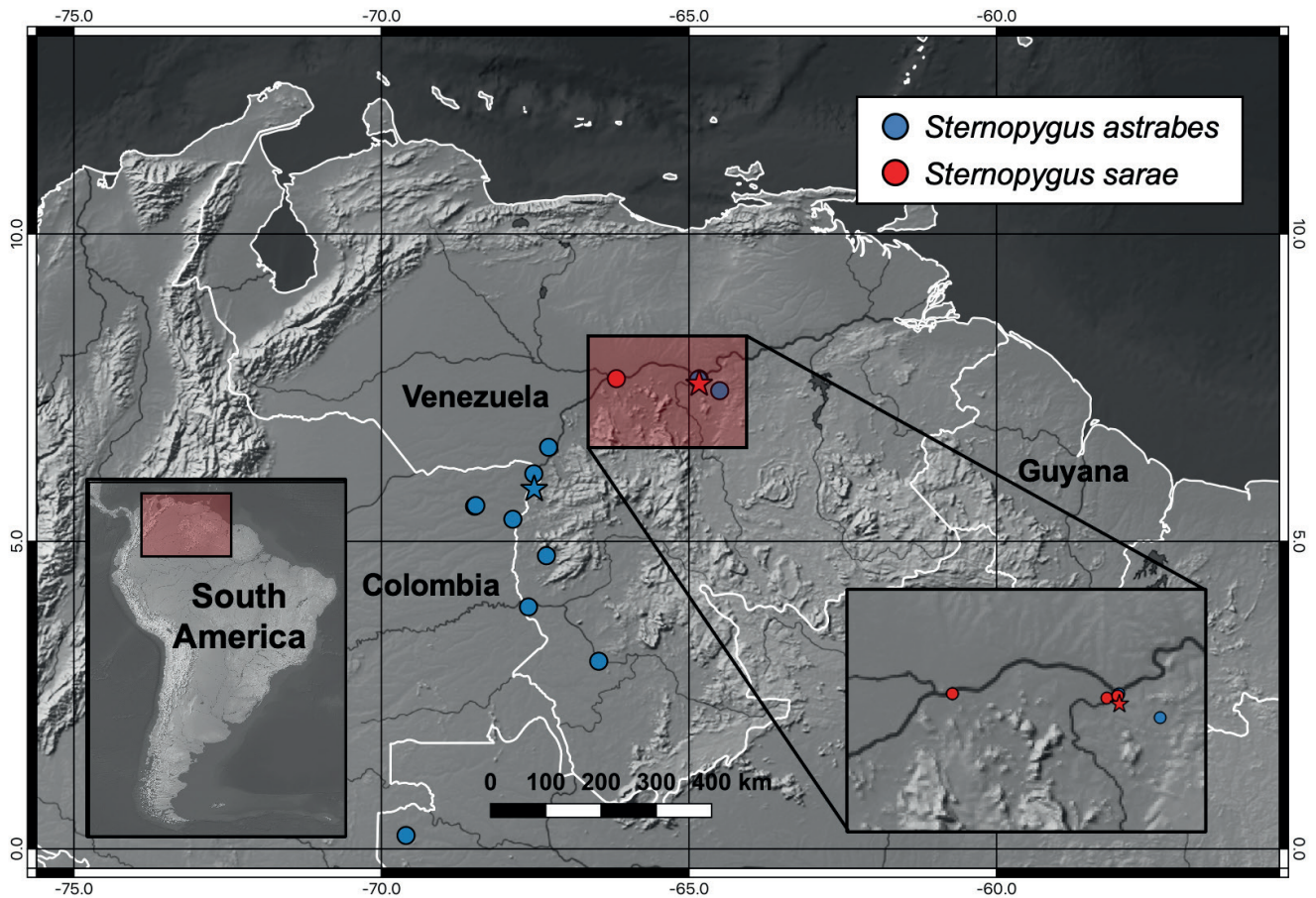


FIGURE 14 | Locality collection map of all known lots of *Sternopygus sarae* (red) and selected *S. astrabes* (blue) lots from the Orinoco River drainage. Holotypes indicated by a star. Symbols may represent more than one collection.

Conservation status. This species is currently known from limited collections in the Orinoco River near the mouth of the Caura River, with an Extension of Occurrence (EOO) calculated by the minimum convex polygon of approximately 1,500 km². As very little is currently known of its actual distribution range or populational trends, and considering existing threats caused by deforestation, extensive agriculture, and gold mining in the region, we suggest the species is preliminarily assessed as Data Deficient (DD) according to the International Union for Conservation of Nature (IUCN) categories and criteria (IUCN Standards and Petitions Subcommittee, 2022).

DISCUSSION

Barred pigment patterns in *Sternopygus*. The alternating darkly pigmented bars and lighter interbars on the lateral body surface of *S. sarae* result from different densities and sizes of chromatophores. These patterns are sometimes more easily discerned when observed closely with a hand lens than at a distance; compare Figs. 3 and 8. The pigmented bars of *S. sarae* from the lower Orinoco River extend to the base of the pterygiophores on the lateral body surfaces, as compared to pigment saddles that do not extend to base of the pterygiophores in juvenile *S. obtusirostris* from the Amazon River, juvenile *S. sabaji* from Atlantic drainages of the Guiana Shield, and *S. astrabes* from lowlands around the Guiana Shield (Fig. 1). The pigment bars are regularly arranged in most specimens of *S. sarae* and are less regularly formed in some specimens (Fig. 9). The high proportion of specimens with 2–4 regular pigment bars/interbars relative to those with inconsistent pigment patterns supports the claim that the chromatophores are largely arranged in vertical bars and not irregular blotches in *S. sarae*. The appearance of these bars in life is presently unknown as this species is not known to have been photographed with live coloration.

The dark saddles of live juvenile *S. obtusirostris* become very conspicuous at night. At this time the interbars become extremely pallid, due to chromatophore contraction. In contrast, juveniles of *S. obtusirostris* are uniformly black and the bars not visible at all during the day (Crampton *et al.*, 2004, fig. 5). Likewise, the dark bars of *S. astrabes* from both the Central Amazon of Brazil and the Rio Orinoco of Venezuela are much more clearly visible in live specimens at night (W. Crampton, 2023, pers. comm.). These observations suggest that variation in the time of day that specimens are captured and fixed (*i.e.*, day *vs.* night) may influence the intensity of dark bars in *Sternopygus*. Likewise, as specimens become more generally faded with time, the dark bars may become harder to discern.

To date, little attention has been given to the phylogenetic distribution of dark vertical bars in *Sternopygus*, or to the evolutionary or adaptive reasons for such a pigment pattern. A future genus-wide phylogenetic analysis will allow us to infer relationships amongst these species with similar pigment patterns, but such an analysis lies outside the scope of this description.

Body shape differences. Body shape differences between *S. sarae* and its sympatric congeners (Fig. 4) may be consistent with predictions of the impedance matching hypothesis of Hopkins (1999). This hypothesis predicts a shorter, thicker electric organ in high-conductivity whitewaters, and a longer, thinner organ in low conductivity black and clearwaters. *Sternopygus sarae* from the sediment-rich, white water Orinoco River, has a longer, less-tapered body than does *S. astrabes* from sediment-poor black and clear water rivers of the Guiana Shield (Fig. 15). It is interesting to note that the more eurytopic *S. macrurus*, which inhabits wide range of water types, also has a wider range of HL, BD, and TR values, and multimodal distributions of these values.

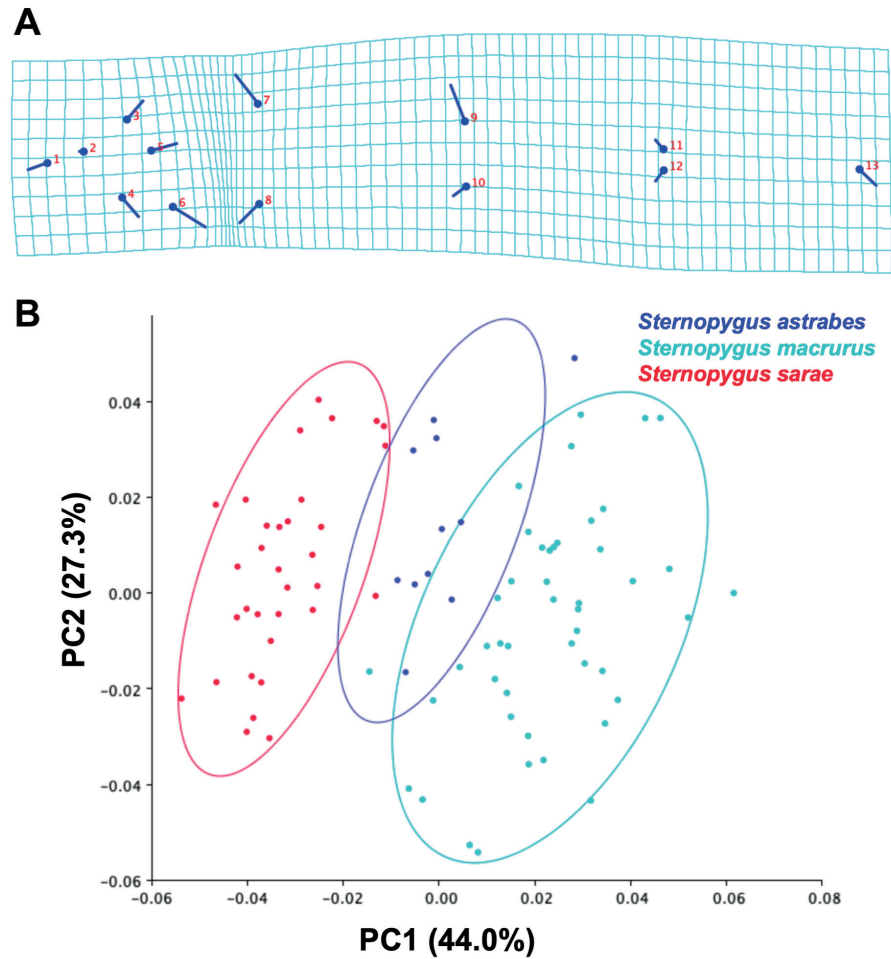


FIGURE 15 | Body-shape variation and diversity in 91 specimens representing three sympatric species of *Sternopygus* from the Guiana Shield. **A.** PC1 transformation grid of all 91 specimens. Ball-and-stick icons indicate direction of variance with balls indicating lower PC1 values. **B.** Morphospace of the first two PCs accounting for 71.3% of total body shape variance. Note: Relatively little overlap in the morphospace occupied by each taxon, indicating that each of these named species possesses a distinct body shape. The species do not separate on PC2. PC2 is not interpreted to be biologically relevant.

Comparative material examined. *Archolaemus blax* Korringa, 1970: **Brazil:** INPA 5064, 1, 380 mm TL. *Archolaemus janeae* Vari, de Santana & Wosiacki, 2012: **Brazil:** ANSP 194705, 2, 214.0–252 mm TL. ANSP 198161, 1, 229 mm TL. *Japigny kirschbaum*: **Guyana:** BMNH 1972.10.17.519, 1, 173.0 mm TL. FMNH 50185, 5, 93.0–182.0 mm TL. FMNH 94511, 1, 162.0 mm TL. FMNH 94512, 1, 158.0 mm TL. *Sternopygus aequilabiatus*: **Colombia:** BMNH 1909.7.23.36–37, 2, 193.0–261.0 mm TL. *Sternopygus arenatus*: **Ecuador:** BMNH 2022.2.30.2–3, 1, 353.0 mm TL. *Sternopygus astrabes*: **Venezuela:** ANSP 162128, 1, 104.0 mm TL, paratype. ANSP 162663, 4, 75.0–237.0 mm TL. INHS 61503, 10, 104.0–226.0 mm TL. *Sternopygus dariensis* Meek & Hildebrand, 1916: **Colombia:** NRM 27742, 1, 387.0 mm TL. NRM 27746, 4, 270.0–349.0 mm TL. **Panama:** UF 12978, 2, 247.0–265.0 mm TL. UF 27523, 6, 109.0–274.0 mm TL. *Sternopygus macrurus*: **Brazil:** MCP 18171, 1, 146.0 mm TL. MCP 22565, 1, 182.0 mm TL. MCP 28932, 1, 171.0 mm TL. MCP 28933, 1, 130.0 mm TL. MCP 30483, 1, 181.0 mm TL. MCP 39921, 1, 83.0 mm TL. MCP 39935, 1, 229.0 mm TL.

MCP 39937, 1, 192.5 mm TL. MCP 39944, 1, 176.0 mm TL. MCP 39947, 1, 261.0 mm TL. MCP 39955, 1, 143.0 mm TL. MCP 39963, 1, 134.0 mm TL. MCP 39972, 1, 119.0 mm TL. MCP 39978, 1, 85.0 mm TL. MCP 39980, 1, 89.0 mm TL. MCP 39983, 1, 124.0 mm TL. MCP 39992, 1, 196.0 mm TL. MCP 39996, 1, 152.0 mm TL. MCP 41125, 1, 107.0 mm TL. **Colombia:** CZUT-IC5325, 1, 575.0 mm TL. IAvH-P-2918, 1, 141.0 mm TL. IAvH-P-3206, 1, 392.0 mm TL. IAvH-P-1838, 1, 116.0 mm TL. IAvH-P-9242, 1, 334.0 mm TL. IAvH-P-7639, 1, 364.0 mm TL. IAvH-P-11293, 2, 241.0–322.0 mm TL. IAvH-P-14311, 1, 149.0 mm TL. IAvH-P-17082, 1, 58.0 mm TL. IAvH-P-17339, 1, 90.0 mm TL. IAvH-P-17499, 1, 78.0 mm TL. IAvH-P-17577, 1, 299.0 mm TL. IAvH-P-17637, 1, 207.0 mm TL. IAvH-P-18393, 1, 96.0 mm TL. IAvH-P-18869, 1, 380.0 mm TL. IAvH-P-19935, 1, 105.0 mm TL. IAvH-P-19568, 1, 107.0 mm TL. IAvH-P-19782, 1, 189.0 mm TL. IAvH-P-20159, 1, 140.0 mm TL. IAvH-P-20170, 1, 193.0 mm TL. IAvH-P-22113, 1, 365.0 mm TL. IAvH-P-22722, 3, 182.0–223.0 mm TL. IAvH-P-22846, 1, 135.0 mm TL. UF 17210, 1, 188.0 mm TL. **French Guiana:** BMNH 1926.3.2.652–5, 656–7, 4, 204.0–382.0 mm TL. FMNH 94816, 5, 172.0–326.0 mm TL. **Paraguay:** NRM 23196, 1, 155.0 mm TL. **Peru:** UF 13196, 1, 232.0 mm TL. UF 116550, 1, 535.0 mm TL. UF 122829, 1, 176.0 mm TL. UF 129338, 1, 228.0 mm TL. **Suriname:** BMNH 1981.6.993–994, 2, 228.0–455.0 mm TL. FMNH 94813, 5, 128.0–250.0 mm TL. FMNH 94814, 5, 213.0–340.0 mm TL. FMNH 94815, 5, 129.0–196.0 mm TL. UF 16268, 1, 197.0 mm TL. **Venezuela:** ANSP 135791, 7, 112.0–266.0 mm TL. ANSP 139497, 1, 226.0 mm TL. ANSP 141594, 1, 168.0 mm TL. ANSP 146197, 2, 131.0–182.0 mm TL. ANSP 149844, 3, 410.0–511.0 mm TL. ANSP 160414, 1, 370.0 mm TL. ANSP 162298, 6, 143.0–398.0 mm TL. ANSP 165737, 1, 269.0 mm TL. ANSP 166820, 1, 189.0 mm TL. ANSP 166830, 1, 184.0 mm TL. ANSP 166831, 1, 345.0 mm TL. ANSP.166833, 2, 486.0–510.0 mm TL. ANSP 167994, 2, 162.0–170.0 mm TL. ANSP 167995, 1, 256.0 mm TL. ANSP 189024, 1, 430.0 mm TL. ANSP 190762, 1, 152.0 mm TL. ANSP 199046, 1, 196.0 mm TL. ANSP 199752, 1, 120.0 mm TL. AUM 36513, 3, 352.0–526.0 mm TL. AUM 43195, 1, 418.0 mm TL. AUM 44097, 1, 236.0 mm TL. AUM 54391, 1, 228.0 mm TL. INHS 97059, 2, 455.0–458.0 mm TL. UF 37028, 3, 149.0–193.0 mm TL. UF 42030, 2, 160.0–194.0 mm TL. UF 80888, 2, 170.0–202.0 mm TL. *Sternopygus obtusirostris:* **Brazil:** INPA 6430, 1, 567.0 mm TL. *Sternopygus pejeraton* Schultz, 1949: **Venezuela:** UMMZ 157671, 2, 165.0–198.0 mm TL, paratypes. *Sternopygus sabaji:* **Guyana:** BMNH 1972.10.17.470–473, 4, 210.0–357.0 mm TL. BMNH 1972.10.17.475–496, 5, 236.0–294.0 mm TL. BMNH 1972.10.17.497–518, 5, 216.0–287.0 mm TL. FMNH 53302, 1, 267.0 mm TL. FMNH 53303, 1, 236.0 mm TL. FMNH 53304, 1, 158.0 mm TL. FMNH 53299, 2, 173.0–239.0 mm TL. FMNH 79693, 5, 112.0–193.0 mm TL. FMNH 105213, 1, 106.0 mm TL. **Suriname:** ANSP 208090, 1, 374.0 mm TL, holotype. ANSP 189018, 17, 46.0–356.0 mm TL, paratypes. FMNH 146152, 7, 98.0–372.0 mm TL, paratypes. *Sternopygus xingu:* **Brazil:** INPA 6425, 1, 361.0 mm TL. INPA 6426, 1, 462.0 mm TL. LBP 2986, 2, 315.0–465.0 mm TL. UMMZ 228961, 2, 206.0–221.0 mm TL, paratypes. *Sternopygus* sp.: **Brazil:** ANSP 197343, 1, 176.0 mm TL. ANSP 197633, 1, 347.0 mm TL. **Suriname:** NRM 33474, 2, 103.0–181.0 mm TL. **Venezuela:** ANSP 182788, 2, 104.0–197.0 mm TL. AUM 43140, 1, 117.0 mm TL. AUM 43196, 1, 493.0 mm TL. AUM 43641, 1, 437.0 mm TL. AUM 53699, 1, 439.0 mm TL.

ACKNOWLEDGMENTS

We thank the following people for their help with arranging loans and access to the specimens used in this description: Mark Sabaj and Mariangeles Arce (ANSP), Caleb McMahan (FMNH), Chris Taylor and Enrique Santoyo-Brito (INHS), David Werneke (AUM), Oliver Crimmen and James Maclaine (BMNH). We also thank Kory Evans for allowing us to use his micro-CT scanner and space in his lab at Rice University. We thank Francisco Provenzano for comments on the type locality and collection

of the specimens, Jessé Figueiredo-Filho for help with photographing the holotype, and Alyx Hebert for preparing and photographing specimens used in the 2D GMM analysis. KTT thanks his wife Madeline for her continued support. JSA thanks his wife Sara for her perennial support. We are very grateful to the Associate Editor, William Crampton, for his thorough review and insights which improved the quality of the manuscript. This research was funded in part by a university doctoral fellowship from the University of Louisiana at Lafayette to KTT, by US National Science Foundation DEB awards 0614334, 0741450, and 1354511 to JSA, and by the Conselho Nacional de Desenvolvimento Científico e Tecnológico (CNPq) awards 306455/2014–5 and 400166/2016–0 to RER.

REFERENCES

- **Adriaens D, Verraes W.** Ontogeny of the osteocranium in the African catfish, *Clarias gariepinus* Burchell (1822) (Siluriformes: Clariidae): ossification sequence as a response to functional demands. *J Morphol.* 1998; 235(3):183–237. [https://doi.org/10.1002/\(SICI\)1097-4687\(199803\)235:3<183::AID-JMOR2>3.0.CO;2-8](https://doi.org/10.1002/(SICI)1097-4687(199803)235:3<183::AID-JMOR2>3.0.CO;2-8)
- **Albert JS, Fink WL.** *Sternopygus xingu*, a new species of electric fish from Brazil (Teleostei: Gymnotoidei), with comments on the phylogenetic position of *Sternopygus*. *Copeia.* 1996; 1996(1):85–102. <https://doi.org/10.2307/1446944>
- **Albert JS.** Species diversity and phylogenetic systematics of American knifefishes (Gymnotiformes, Teleostei). *Misc Publ Mus Zool. University of Michigan.* 2001; (190):1–129.
- **Albert JS, Crampton WGR.** Diversity and phylogeny of Neotropical electric fishes (Gymnotiformes). In: Bullock TH, Hopkins CD, popper AN, Fay RR, editors. *Electroreception. Springer Handbook of Auditory Research.* 2005; 21:360–409. https://doi.org/10.1007/0-387-28275-0_13
- **Albert JS, Crampton WGR, Thorsen DH, Lovejoy NR.** Phylogenetic systematics and historical biogeography of the Neotropical electric fish *Gymnotus* (Teleostei: Gymnotidae). *Syst Biodivers.* 2005; 2(4):375–417. <https://doi.org/10.1017/S1477200004001574>
- **Albert JS, Petry P, Reis RE.** Major biogeographic and phylogenetic patterns. In: Albert JS, Reis RE, editors. *Historical Biogeography of Neotropical freshwater fishes.* University California Press; 2011. p.21–57.
- **Albert JS, Tagliacollo VA, Dagosta FCP.** Diversification of Neotropical freshwater fishes. *Annu Rev Ecol Evol S.* 2020; 51(1):27–53. <https://doi.org/10.1146/annurev-ecolsys-011620-031032>
- **Arratia G.** Morphology, taxonomy, and phylogeny of Triassic pholidophorid fishes (Actinopterygii, Teleostei). *J Vertebr Paleontol.* 2013; 33:1–38. <https://doi.org/10.1080/02724634.2013.835642>
- **Barbarino Duque A, Winemiller KO.** Dietary segregation among large catfishes of the Apure and Arauca Rivers, Venezuela. *J Fish Biol.* 2003; 63(2):410–27. <https://doi.org/10.1046/j.1095-8649.2003.00163.x>
- **Brejão GL, Gerhard P, Zuanon J.** Functional trophic composition of the ichthyofauna of forest streams in eastern Brazilian Amazon. *Neotrop Ichthyol.* 2013; 11(2):361–73. <https://doi.org/10.1590/S1679-62252013005000006>
- **Buser TJ, Boyd OF, Cortés A, Donatelli CM, Kolmann MA, Luparell JL et al.** The natural historian's guide to the CT galaxy: step-by-step instructions for preparing and analyzing computed tomographic (CT) data using cross-platform, open access software. *Integr Org Biol.* 2020; 2(1):obaa009. <https://doi.org/10.1093/iob/obaa009>
- **Crampton WGR.** Gymnotiform fish: an important component of Amazonian floodplain fish communities. *J Fish Biol.* 1996; 48(2):298–301. <https://doi.org/10.1111/j.1095-8649.1996.tb01122.x>
- **Crampton WGR.** Effects of anoxia on the distribution, respiratory strategies and electric signal diversity of gymnotiform fishes. *J Fish Biol.* 1998a; 53:307–30. <https://doi.org/10.1111/j.1095-8649.1998.tb01034.x>

- **Crampton WGR.** Electric signal design and habitat preferences in a species rich assemblage of gymnotiform fishes from the Upper Amazon basin. *An Acad Bras Cienc.* 1998b; 70(4):805–47.
- **Crampton WGR, Hulen KG, Albert JS.** *Sternopygus branco*: a new species of Neotropical electric fish (Gymnotiformes: Sternopygidae) from the lowland Amazon basin, with descriptions of osteology, ecology, and electric organ discharges. *Copeia.* 2004a; 2004(2):245–59. <https://doi.org/10.1643/CI-03-105R1>
- **Crampton WGR.** Diversity and adaptation in deep-channel Neotropical electric fishes. In: Sebert P, Onyango DW, Kapoor BG, editors. *Fish Life in Special Environments.* Science Publishers, Enfield, NH; 2007. p.283–339.
- **Crampton WGR.** An ecological perspective on diversity and distributions. In: Albert JS, Reis RE, editors. *Historical Biogeography of Neotropical Freshwater Fishes.* University of California Press, Berkeley; 2011. p.165–89.
- **Crampton WGR, Hulen KG, Albert JS.** Redescription of *Sternopygus obtusirostris* (Gymnotiformes: Sternopygidae) from the Amazon basin, with description of osteology, ecology and electric organ discharges. *Ichthyol Explor Freshw.* 2004b; 15(2):121–34.
- **Eigenmann CH, Allen WR.** Fishes of western South America. I. The intercordilleran and Amazonian lowlands of Peru. II. The high pampas of Peru, Bolivia, and northern Chile. University of Kentucky; 1942.
- **Eigenmann CH, Ward DP.** The Gymnotidae. *J Wash Acad.* 1905; 159–88.
- **Fedorov A, Beichel R, Kalpathy-Cramer J, Finet J, Fillion-Robin JC, Pujol S et al.** 3D Slicer as an image computing platform for the Quantitative Imaging Network. *Mag Reson Imaging.* 2012; 30(9):1323–41. <https://doi.org/10.1016/j.mri.2012.05.001>
- **Fernandes CC.** Detrended canonical correspondence analysis (DCCA) of the electric fish assemblages in the Amazon. In: Val AL, Almeida-Val VMF, editors. *Proceedings of the International Symposium of Biology of Tropical Fishes.* Instituto Nacional de Pesquisas da Amazônia; 1999. p.21–39.
- **Fink SV, Fink WL.** Interrelationships of the ostariophysan fishes (Teleostei). *Zoo J Linn Soc-Lond.* 1981; 72(4):297–353. <https://doi.org/10.1111/j.1096-3642.1981.tb01575.x>
- **Heiligenberg W.** *Neural Nets in Electric Fish (Computational Neuroscience).* MIT press; 1991.
- **Hopkins CD.** Design features for electric communication. *J Exp Biol.* 1999; 202(10):1217–28.
- **Hulen KG, Crampton WGR, Albert JS.** Phylogenetic systematics and historical biogeography of the neotropical electric fish *Sternopygus* (Teleostei: Gymnotiformes). *System Biodivers.* 2005; 3(4):407–32. <https://doi.org/10.1017/S1477200005001726>
- **International Union for Conservation of Nature (IUCN). Standards and Petitions Committee.** Guidelines for Using the IUCN Red List Categories and Criteria. Version 15.1 [Internet]. 2022. Available from: <https://www.iucnredlist.org/documents/RedListGuidelines.pdf>
- **Klingenberg CP.** MorphoJ: an integrated software package for geometric morphometrics. *Mol Ecol Resour.* 2011; 11(2):353–57. <https://doi.org/10.1111/j.1755-0998.2010.02924.x>
- **Lasso CA, Mojica JI, Usma JS, Maldonado JA, DoNascimento C, Taphorn DC et al.** Peces de la cuenca del río Orinoco. Parte I: Lista de especies y distribución por subcuencas. *Biota Colombiana.* 2004; 5(2):95–157.
- **Lasso CA, Rial A, Matallana CL, Ramírez W, Celsa Señaris J, Díaz-Pulido A et al.** Biodiversidad de la cuenca del Orinoco: II. Áreas prioritarias para la conservación y uso sostenible. Instituto de Investigación de Recursos Biológicos Alexander von Humboldt; 2011.
- **Lasso CA, Machado-Allison A, Taphorn DC.** Fishes and aquatic habitats of the Orinoco River Basin: diversity and conservation. *J Fish Biol.* 2016; 89(1):174–91. <https://doi.org/10.1111/jfb.13010>
- **Lovejoy NR, Lester K, Crampton WGR, Marques FP, Albert JS.** Phylogeny, biogeography, and electric signal evolution of Neotropical knifefishes of the genus *Gymnotus* (Osteichthyes: Gymnotidae). *Mol Phylogenet Evol.* 2010; 54(1):278–90. <https://doi.org/10.1016/j.ympev.2009.09.017>

- **Lundberg JG, Stager JC.** Microgeographic diversity in the Neotropical knife-fish *Eigenmannia macrops* (Gymnotiformes, Sternopygidae). *Environ Biol Fish.* 1985; 13(3):173–81. <https://doi.org/10.1007/BF00000928>
- **Lundberg JG, Lewis Jr WM, Saunders III JF, Mago-Leccia F.** A major food web component in the Orinoco River channel: evidence from planktivorous electric fishes. *Science.* 1987; 237(4810):81–83. <https://doi.org/10.1126/science.237.4810.81>
- **Lundberg JG, Mago-Leccia F.** A review of *Rhabdolichops* (Gymnotiformes, Sternopygidae), a genus of South American freshwater fishes, with descriptions of four new species. *Proc Acad Nat Sci Phila.* 1986:53–85.
- **Machado-Allison A.** Los peces de los llanos de Venezuela: Un ensayo sobre su Historia Natural. Caracas: Universidad Central de Venezuela, Consejo de Desarrollo Científico y Humanístico; 1987.
- **Mago-Leccia F.** Los peces de la familia Sternopygidae de Venezuela. *Acta Cient Venez.* 1978; 29:1–89.
- **Mago-Leccia F.** Electric fishes of the continental waters of America. Classification and catalogue of the electric fishes of the order Gymnotiformes (Teleostei: Ostariophysi), with descriptions of new genera and species. Caracas: Fundacion para el Desarrollo de las Ciencias Fisicas, Matematicas y Naturales; 1994.
- **Maldonado-Ocampo JA, Albert JS.** Species diversity of gymnotiform fishes (Gymnotiformes, Teleostei) in Colombia. *Biota Colomb.* 2003; 4(2):147–65. Available from: <https://www.redalyc.org/pdf/491/49140202.pdf>
- **Maldonado-Ocampo JA.** Filogenia molecular da família Sternopygidae (Gymnotiformes: Sternopygoidei). [PhD Thesis]. Rio de Janeiro: Universidade Federal do Rio de Janeiro; 2011.
- **Marceniuk AP, Caires RA, Rotundo MM, Alcantara RAK, Wosiacki WB.** The ichthyofauna (Teleostei) of the Rio Caeté estuary, northeast Pará, Brazil, with a species identification key from northern Brazilian coast. *Pan-Am J Aquat Sci.* 2017; 12(1):31–79. Available from: [http://panamjas.org/pdf_artigos/PANAMJAS_12\(1\)_31-79.pdf](http://panamjas.org/pdf_artigos/PANAMJAS_12(1)_31-79.pdf)
- **Marrero C, Winemiller KO.** Tube-snouted gymnotiform and mormyriiform fishes: convergence of a specialized foraging mode in teleosts. *Environ Biol Fish.* 1993; 38(4):299–309. <https://doi.org/10.1007/BF00007523>
- **Meunier FJ, Jégu M, Keith P.** A new genus and species of neotropical electric fish, *Japigny kirschbaum* (Gymnotiformes: Sternopygidae), from French Guiana. *Cybium.* 2011; 35(1):47–53.
- **Peixoto LAW, Waltz BT.** A new species of the *Eigenmannia trilineata* (Gymnotiformes: Sternopygidae) species group from the río Orinoco basin, Venezuela. *Neotrop Ichthyol.* 2017; 15(1):e150199. <https://doi.org/10.1590/1982-0224-20150199>
- **Rohlf FJ.** *TPSUtil, v. 1.40.* NY: State University at Stony Brook; 2008.
- **Sabaj MH.** Codes for Natural History Collections in Ichthyology and Herpetology. *Copeia.* 2020; 108(3):593–669. <https://doi.org/10.1643/ASIHCONDONS2020>
- **Santos Silva D, Milhomem SSR, Souza ACP, Pieczarka JC, Nagamachi CY.** A conserved karyotype of *Sternopygus macrurus* (Sternopygidae, Gymnotiformes) in the Amazon region: differences from other hydrographic basins suggest cryptic speciation. *Micron.* 2008; 39(8):1251–54. <https://doi.org/10.1016/j.micron.2008.04.001>
- **Schindelin J, Arganda-Carreras I, Frise E, Kaynig V, Longair M, Pietzsch T et al.** Fiji: an open-source platform for biological-image analysis. *Nat Methods.* 2012; 9(7):676–82. <https://doi.org/10.1038/nmeth.2019>
- **Torgersen KT, Albert JS.** A new species of *Sternopygus* (Gymnotiformes: Sternopygidae) from the Atlantic Coast of the Guiana Shield. *Ichthyology & Herpetology.* 2022; 110(4):714–27. <https://doi.org/10.1643/i2022013>
- **Triques ML.** *Sternopygus castroi*, a new species of Neotropical freshwater electric fish, with new synapomorphies to the genus (Sternopygidae: Gymnotiformes: Teleostei). *Stud Neotrop Fauna E.* 2000; 35(1):19–26.
- **Unguez GA, Zakon HH.** Phenotypic conversion of distinct muscle fiber populations to electrocytes in a weakly electric fish. *J Comp Neurol.* 1998; 399(1):20–34. [https://doi.org/10.1002/\(SICI\)1096-9861\(19980914\)399:1<20::AID-CNE2>3.0.CO;2-C](https://doi.org/10.1002/(SICI)1096-9861(19980914)399:1<20::AID-CNE2>3.0.CO;2-C)

- **Van der Sleen P, Albert JS.** Field guide to the fishes of the Amazon, Orinoco, and Guianas. Princeton University Press; 2017.
- **Vari RP, Ferraris Jr CJ, Radosavljevic A, Funk VA.** Checklist of the freshwater fishes of the Guiana Shield. Proc Biol Soc Wash. 2009; 17(1). <https://doi.org/10.2988/0097-0298-17.1.i>
- **Waddell JC, Crampton WGR.** A simple procedure for assessing sex and gonadal maturation in gymnotiform fish. Aqua Intern J Ichthyol. 2018; 24(1):1–08.
- **Waddell JC, Njeru SM, Akhiyat YM, Schachner BI, Correa-Roldán EV, Crampton WGR.** Reproductive life-history strategies in a species-rich assemblage of Amazonian electric fishes. PLoS ONE. 2019; 14(12):e0226095. <https://doi.org/10.1371/journal.pone.0226095>
- **Waltz BT, Albert JS.** Family Sternopygidae: Glass knifefishes, rattail knifefishes. In: Van der Sleen P, Albert JS, editors. Field guide to the fishes of the Amazon, Orinoco and Guianas. Princeton University Press; 2017. p.341–45.
- **Wilke CO.** ggrridges: ridgeline plots in 'ggplots2'. R package version 0.5. 2018; 1.
- **Winemiller KO.** Floodplain river food webs: generalizations and implications for fisheries management. In: Proceedings of the Second International Symposium on the Management of Large Rivers for Fisheries; 2004. p.285–309.

AUTHORS' CONTRIBUTION

Kevin T. Torgersen: Conceptualization, Data curation, Formal analysis, Investigation, Methodology, Project administration, Writing–original draft, Writing–review and editing.

Aleidy M. Galindo-Cuervo: Investigation, Resources, Validation, Writing–review and editing.

Roberto E. Reis: Funding acquisition, Writing–review and editing.

James S. Albert: Formal analysis, Funding acquisition, Investigation, Methodology, Resources, Supervision, Validation, Writing–original draft, Writing–review and editing.

ETHICAL STATEMENT

Not applicable.

COMPETING INTERESTS

The author declares no competing interests.

HOW TO CITE THIS ARTICLE

- **Torgersen KT, Galindo-Cuervo AM, Reis RE, Albert JS.** A new species of barred *Sternopygus* (Gymnotiformes: Sternopygidae) from the Orinoco River. Neotrop Ichthyol. 2023; 21(1):e220088. <https://doi.org/10.1590/1982-0224-2022-0088>



This is an open access article under the terms of the Creative Commons Attribution License, which permits use, distribution and reproduction in any medium, provided the original work is properly cited.

Distributed under Creative Commons CC-BY 4.0

© 2023 The Authors. Diversity and Distributions Published by SBI



Official Journal of the
Sociedade Brasileira de Ictiologia